

8

Carbon nanotubes membranes

Toraj Mohammadi*, Maryam Ahmadzadeh Tofighy

Research and Technology Centre for Membrane Processes, Faculty of Chemical Engineering, Iran University of Science and Technology (IUST), Narmak, Tehran, Iran

*Corresponding author

Outline:

INTRODUCTION.....	181
CARBON NANOTUBES (CNTS)	183
Basic CNTs information.....	183
Nanofluidics of CNTs membranes.....	184
Functionalization of CNTs.....	186
<i>Defect functionalization</i>	186
<i>Non-covalent functionalization</i>	186
<i>Covalent functionalization</i>	186
CNTs MEMBRANES.....	187
Types of CNTs membranes.....	187
<i>Vertically aligned CNTs membranes</i>	189
<i>Mixed (composite) CNTs membranes</i>	190
Fabrication of CNTs membranes	190
<i>Alignment and filling of CNTs</i>	191
<i>Functionalization and grafting of CNTs</i>	195
CNTs MEMBRANE FOR SEPARATION.....	197
Gas separation by CNTs membranes.....	197
Liquid separation and pervaporation (PV) by CNTs membranes.....	201
CONCLUSION.....	208
REFERENCES.....	209

Introduction

Carbon nanotubes (CNTs), either single walled carbon nanotubes (SWCNTs) or multi walled carbon nanotubes (MWCNTs), have received increasing attention due to their unique structural and extraordinary chemical and physical properties and wide range of applications over other materials. CNTs have unique combination of mechanical (Young's modulus ~ 1 TPa and tensile strength up to 60 GPa, which can be more than 100 times that of stainless steel), electrical (maximum electrical conductivity at 300K $\sim 10^6$ S/m for SWNT and $>10^5$ S/m for MWNT, which makes them excellent conductors – comparable to copper – or semiconductors) and thermal properties (maximum thermal conductivity of 6600 W/mK for an individual SWNT and > 3000 W/mK for an individual MWNT comparable to diamond) as well as low density, flexibility, thermal stability as high as 2000–2400 °C in an argon atmosphere or under vacuum and large aspect ratio (diameter as low as 3.3 Å and length as high as 6 mm, commercially available CNTs have diameters \sim nm and lengths \sim mm, therefore aspect ratio has an order of 10^2) and their ability to establish different types of interactions with organic and inorganic analytes. In fact, they have even been designated in several occasions as the most researched materials of the 21st century [1-12].

CNTs have been synthesized by various methods, e.g. electric arc discharge, laser ablation and chemical vapor deposition (CVD). CVD appears to be a promising method to synthesize CNTs because of its low cost, simple configuration and high flexibility in adjustable parameters for controlling the CNTs structures [13-16].

Membrane science has grown synergistically over the past thirty years. Increasing energy issue has become important and its rising cost is probably one of the reasons for membrane technology to play an influential role in reducing the environmental impacts. Membranes are promising candidates for separation due to their high stability and efficiency, low operating and capital cost, low energy requirement and also ease of operation. Membranes with good thermal and mechanical stability combined with good solvent resistance can be suitable for industrial processes. Furthermore, they are also known for their reliability to be used in remote locations as membranes have no moving parts and thus making them mechanically robust. Membrane-based separations have demonstrated outstanding advantages over the conventional separation methods such as adsorption and distillation which involve troublesome and complicated operations. Nowadays, membrane-based separation has been widely applied in the industrial scale for gas separation, liquid separation and pervaporation. The current applications of membrane-based gas separation include removal of carbon dioxide from fuel or flue gas, hydrogen recovery and natural gas separation. On the other hand, the application of membrane-based liquid separation has been extended to ultra/microfiltration and reverse osmosis [17-20].

The growing interest has led to development of inorganic and polymeric membranes. Polymeric membranes are either porous or dense and have low mechanical stability. They often show reduced permeate flux at higher pressure. This reduction may result from compaction of the originally porous structure to the more dense structure. Generally, inorganic membranes can provide the desired material properties for different separation processes. However, their performance and higher cost compared to polymeric membranes may restrict their industrial applications. Development of novel membrane architecture today is of great importance to enhance the membrane performance in separation. The recent development of polymeric and inorganic materials has seemingly reached a limit in trade-off between selectivity and permeability. The deficiencies of these materials have in turn switched the focus of researches towards the realization of a new class of membranes, namely mixed matrix membranes (MMMs). MMMs comprise an inorganic entities embedded in a polymer matrix and have been proposed as an

alternative approach to obtain promising selectivity benefits of the inorganic media with economical processing capabilities of polymers [21].

Water, a nonsubstitutional natural resource, has been already scarce, and is becoming increasingly scarce day by day. Due to population growth, economic development, rapid urbanization, large-scale industrialization and environmental concerns, water stress has emerged as a real threat. Additionally, climate aberrance has significantly affected water stress, changed rainfall patterns, and shrunked snow and ice covers that feed rivers. While scarcity drives us to use lower quality and unconventional water sources, membrane separation technology can meet these global climate challenges. Membranes are widely used not only to treat surface water but also to reuse wastewater and to desalinate seawater which can alleviate the problem of water scarcity. However, one of the main problems with desalination membrane technology is the high level of energy consumption. For example, the energy consumption for seawater desalination using reverse osmosis (RO) membranes has dropped from 8.0 to 3.4 kWh/m³. Advanced energy recovery devices are expected to be available soon, and the specific energy consumption (SEC) is being decreased to <2.5 kWh/m³. Nevertheless, this consumption is still higher than the theoretically limited value for seawater desalination of 1.06 kWh/m³ (assuming 35,000 mg/L of salt in seawater and a typical recovery of 50%). One key for further decreasing the energy consumption is to develop novel membrane materials with higher permeability. Nevertheless, the current thin film composite (TFC) RO membranes suffer from a trade-off between salt rejection rate and permeability. To overcome the limits of current polymeric membranes, new types of membranes with higher permeability and rejection rate have been invented. These membranes use CNTs as membrane pores. One of the most remarkable properties of CNTs, which makes them attractive for membrane preparation, is their unique combination of extremely high aspect ratio with small dimensions. The second important property of CNTs critical for transport applications is the remarkable atomic scale smoothness and chemical inertness of the graphitic walls. These CNTs membranes could potentially provide a solution to water shortages, as they seem to outperform existing membranes by providing higher water flux and lower energy consumption [22-33].

A number of theoretical reports have considered the behavior of water confined in CNTs [34-43]. Sholl et al. [44] reported simulation results of extremely high gas diffusivity in CNTs and high gas permeability for the vertically aligned CNTs membranes. Hinds et al. [45] and Holt et al. [46] reported synthesis of free-standing and silicon-chip supported vertically aligned CNTs membranes via a complex synthesis method, and confirmed experimentally high permeability for the CNTs membranes. However, it is difficult to use the free-standing or silicon-chip supported CNTs membranes in large-scale industrial applications. Macroporous α -alumina in various geometries is arguably the most common support for inorganic membranes used in commercial applications. Lin et al. [47,48] also reported synthesis of CNTs membrane on porous α -alumina support via a multi-step method. Fornasiero et al. [49] also reported synthesis of vertically aligned CNTs membrane. They did fill the gaps between the CNTs by low pressure silicon nitride deposition, and as a result, the CNTs were only functionalized at their entrances by plasma treatment to control water desalination. Also, Tofighy et al. [50] reported synthesis of vertically aligned CNTs membrane on porous α -alumina support via a simple method for salty water desalination.

In comparison to other membranes, there are only limited works reported on preparation of CNTs membranes for gas or liquid separations. Because, it is impossible to synthesize CNTs membranes with nanotubes inter-grown together without inter-tube gaps, due to the unique structure of single-walled or multi-walled CNTs and their growth mechanisms, hence, filling the inter-tube gaps of CNTs arrays is the main step of the CNTs membrane synthesis. Also, removing the excess filling layer from the CNTs membranes is controversial and difficult.

Therefore, the feasibility of CNTs membranes has not been fully investigated, as they are still in the laboratory stage of development and not yet commercially available. Fabrication of CNTs membranes, with controlled geometry, porosity and pore shapes is also challenging.

Carbon nanotubes (CNTs)

Basic CNTs information

CNTs are rolled-up structures of a perfect hexagonal carbon crystal molecular sheet (graphene, the strongest known material) as tubular cylinders. Since the discovery of CNTs in 1991 by Iijima [1], they have received much attention for their many potential applications, such as nanoelectronic and photovoltaic devices [51,52], superconductors [53], electromechanical actuators [54], electrochemical capacitors [55], nanowires [56] and nanocomposite materials [57,58]. Carbon nanotubes may be classified as single-walled carbon nanotubes (SWCNTs) [59,60], double-walled carbon nanotubes (DWCNTs) [61,62] or multi-walled carbon nanotubes (MWCNTs) [1]. SWCNTs and DWCNTs comprise cylinders of one or two (concentric), respectively, of graphene sheets, whereas MWCNTs consist several concentric cylindrical shells of graphene sheets. CNTs are synthesized in a variety of ways, such as arc discharge [59], laser ablation [63], high pressure carbon monoxide (HiPCO) [64] and chemical vapor deposition (CVD) [65,66]. CNTs exhibit excellent mechanical, electrical, thermal and magnetic properties [67,68]. The exact magnitude of these properties depends on diameter and chirality of the nanotubes and whether they are single-walled, double-walled or multi-walled form. Typical properties of CNTs and graphite are collected in Table 8.1 [69–74].

TABLE 8.1

Theoretical and experimental properties of CNTs and graphite [75]

Property	CNTs	Graphite
Specific gravity	0.8 g/cm ³ for SWCNT; 1.8 g/cm ³ for MWCNT (Theoretical)	2.26 g/cm ³ for
Elastic modulus	~1 TPa for SWCNT; ~0.3-1 TPa for MWCNT;	1 TPa (in-plane)
Strength	50-500 GPa for SWCNT; 10-60 GPa for MWCNT	
Resistivity	5-50 μm	50 μm (in plane)
Thermal conductivity	3000 W m ⁻¹ K ⁻¹ (Theoretical)	3000 W m ⁻¹ K ⁻¹ (in-plane); 6 W m ⁻¹ K ⁻¹ (c-axis)
Magnetic susceptibility	22×10 ⁶ EMU/g (perpendicular with plane); 0.5×10 ⁶ EMU/g (parallel with plane)	
Thermal expansion	Negligible (Theoretical)	-1×10 ⁻⁶ K ⁻¹ (in plane); 29×10 ⁻⁶ K ⁻¹ (c-axis)
Thermal stability	>700 °C (in air); 2800 °C (in vacuum)	450-650 °C (in air)

Because of these excellent properties, CNTs can be used as ideal reinforcing agents for high performance composite materials. The excellent mechanical properties of CNTs arise from the presence of carbon-carbon bond in the graphite layers, which are most probably the strongest chemical bond known in nature. This sp² bonding has eventually contributes to the high stiffness and axial strength of CNTs [76].

The cylindrical shape of a SWNT can be imagined virtually by wrapping it in a layer of graphite called graphene. The way graphene winds can be described by a pair of indices (n, m). The indices n and m are integers indicating the number of unit vectors along two directions of graphene (Figure 8.1) [76]. The inner diameter of a nanotube can be calculated from the “rolled up” vector as follows [77]:

$$d_{in} = \left(\frac{a}{\pi}\right)\sqrt{(n^2 + m^2 + nm)} - 2r_c \quad (1)$$

Where, d_{in} is inner diameter (I.D.) of nanotubes, a is lattice parameter of graphene ($=2.46 \text{ \AA}$) and r_c is vander Waal's radius of a carbon atom (1.7 \AA).

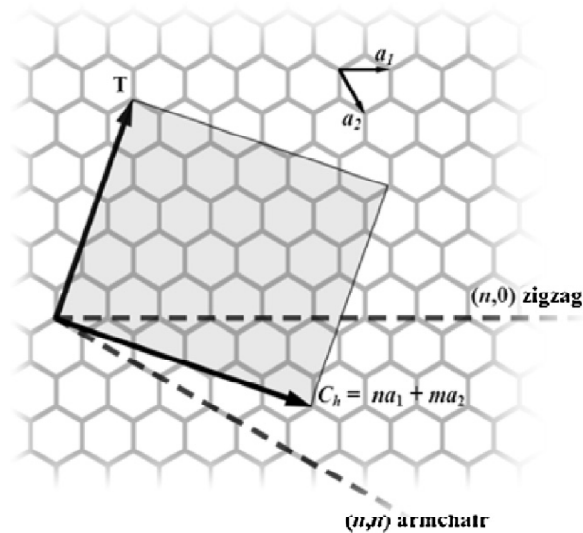


FIGURE 8.1

Letters (n, m) indicate the number of unit vectors in an infinite graphene sheet and C_h is a ‘rolled up’ vector. T denotes the tube axis, and a_1 and a_2 are the unit vectors of graphene. If $m = 0$, the CNTs are called ‘zigzag’. If $n = m$, the CNTs are called ‘armchair’. In other cases, the CNTs are ‘chiral’ [87]

Nanofluidics of CNTs membranes

The inner walls of CNTs are smooth and hydrophobic. Movement of water molecules passing through the interior a CNT can be explained by the ballistic motion of water chains (1D wire) due to strong hydrogen bonding between water molecules and minimal interaction with the CNT inner wall [78–80] (Figure 8.2).

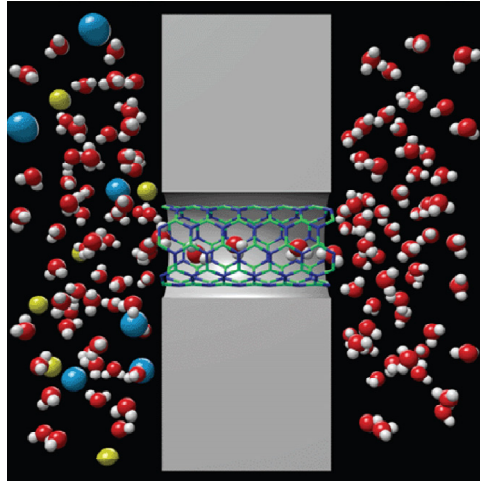


FIGURE 8.2
Movement of water molecules through a SWNT [87]

The mass movement of water molecules through a CNT does not follow conventional fluid mechanics [81]. Thus, it is necessary to introduce a plausible transport phenomenon called “nanofluidics”. In this novel theory, it is assumed that the fluid flowing through a nano-channel has a slip length with no friction [82]. Adopting the slip-flow condition, the Hagen–Poiseuille equation can be used as follows [81]:

$$Q_{slip} = \frac{\pi(d/2)^4 + 4(\frac{d}{2})^3 \cdot L_S(d)}{8\mu} \cdot \frac{\Delta P}{L} \quad (2)$$

Where Q_{slip} is water flux depending on the slip length, d is diameter of the nano-channel, ΔP is pressure difference between both ends of the nano-channel, μ is viscosity of water and L is the length of nano-channel. The slip length ($L_S(d)$) can be computed as follows:

$$L_S(d) = L_{S,\infty} + \frac{C}{d^3} \quad (3)$$

Where $L_{S,\infty}$ is the slip length of the graphene surface (assumed to be 30 nm), and C is a fitting parameter. Additionally, the diffusion coefficient of water molecules is estimated as $D_{H_2O} = 0.9423 \times 10^{-9} \frac{m^2}{s}$ for a 2.1 nm diameter nanotube [83].

In this manner, the CNTs membranes use inner and/or outer surface of CNTs as nano-channels for transporting fluid. With this configuration, applications of the CNTs membranes may not be limited to desalination processes. Additionally, it may be feasible to extend the use of CNTs membranes to include separation technologies for oil and gas [84–86].

Transport of fluids through CNTs is of great interest since they have been recognized as a promising material for nanofluidic and membrane technology. The high fluid fluxes reported in the recent publications are attributed to the atomic-scale smoothness of the CNTs walls and the molecular ordering phenomena inside the nanopores [87].

Functionalization of CNTs

Since CNTs usually agglomerate due to Van der Waals force, they are extremely difficult to disperse and align in a polymer matrix. Thus, a significant challenge in developing high performance polymer/CNTs composites is to introduce the individual CNTs in the polymer matrix in order to achieve better dispersion and alignment and strong interfacial interactions, to improve the load transfer across the CNT-polymer matrix interface. Functionalization of CNTs is an effective way to prevent CNT aggregation, which helps to better disperse and stabilize the CNTs within the polymer matrix. There are several approaches for functionalization of CNTs including defect functionalization, covalent functionalization and non-covalent functionalization [88].

Defect functionalization

CNTs can be purified via oxidative methods by oxygen, air, concentrated sulfuric acid, nitric acid, aqueous hydrogen peroxide, and acid mixture to remove metal particles and/or amorphous carbon from the raw materials (untreated CNTs). In these methods, defects are preferentially observed at the open ends of CNTs. The purified SWNTs contain oxidized carbon atoms in the form of $-\text{COOH}$ group. In these oxidizing methods, SWNTs are broken to very short tubes (pipes) of lengths 100-300nm [89-93].

Surface of the acid treated MWNTs indicates the presence of some defects in the carbon-carbon bonding associated with the formation of carboxylic acid groups on the surface, while the raw MWNTs show uniform surface and a clear diffraction pattern because of their perfect lattice structure of carbon-carbon bonds. The number of $-\text{COOH}$ groups on the surface of CNTs depends on the acid treatment temperature and time, increasing with increasing temperature. The extent of the induced $-\text{COOH}$ and $-\text{OH}$ functionality also depends on the oxidation procedures and oxidizing agents. The CNTs ends can be also opened during the oxidation process [94-100].

Non-covalent functionalization

Non-covalent functionalization of CNTs is of particular interest because it does not compromise the physical properties of CNTs, but improves their solubility and processability. This type of functionalization mainly involves surfactants, biomacromolecules or wrapping with polymers. In the search for non-destructive purification methods, CNTs can be transferred to the aqueous phase in the presence of surfactants [101,102]. In this case, the CNTs are surrounded by the hydrophobic components of the corresponding micelles. The interaction becomes stronger when the hydrophobic part of the amphiphilic contains an aromatic group. CNTs can be well dispersed in water using anionic, cationic and non-ionic surfactants [103-106].

Covalent functionalization

Because of the π -orbitals of the sp^2 -hybridized C atoms, CNTs are more reactive than those with a flat graphene sheet and, and they have an enhanced tendency to covalently attach with chemical species. In the case of covalent functionalization, translational symmetry of CNTs is disrupted by changing sp^2 carbon atoms to sp^3 carbon atoms, and properties of CNTs, such as electronic and transport, are influenced. But this functionalization of CNTs can improve solubility as well as dispersion in solvents and polymers. Covalent functionalization can be accomplished by either modification of surface-bound carboxylic acid groups on the CNTs or by direct reagents to the side

walls of CNTs. Generally, functional groups such as $-\text{COOH}$ or $-\text{OH}$ are created on the CNTs during the oxidation by oxygen, air, concentrated sulfuric acid, nitric acid, aqueous hydrogen peroxide, and acid mixtures. The presence of carboxylic acid groups on the CNT surface is more convenient than others because a variety of chemical reactions can be conducted with this group. The presence of $-\text{COOH}$ or $-\text{OH}$ group on the CNT surface helps attachment of organic [107] or inorganic materials, which is important for solubilizing CNTs. CNTs can be covalently functionalized with thiocarboxylic and dithiocarboxylic esters that help crosslinking between CNTs [108]. CNTs can be also functionalized at the end caps or at the sidewalls to enhance their dispersion as well as solubilization in solvents and in polymer matrices [109]. SWNTs can be fluorinated at their side walls by passing elemental fluorine at different temperatures [110]. The fluorinated SWNTs exhibit improved solubility in isopropanol or dimethylformamide by ultrasonication [111,112]. Fluorinated SWNTs may be converted to side walls alkylated SWNTs by reaction with Grignard reagent or alkyllithium compounds that are soluble in chloroform [113]. SWNTs can also be solubilized by direct functionalization of their side walls by nitrenes [114,115], carbenes [115] and arylation [116,117].

Functionalization of CNTs with polymer molecules (polymer grafting) is particularly important for processing of polymer/CNT nanocomposites [118,119]. Two main categories “grafting to” and “grafting from” approaches have been reported for the covalent grafting of polymers to CNTs. The “grafting to” approach is based on attachment molecules on the CNTs surface by chemical reactions, such as amidation, esterification, radical coupling, etc. The polymer must have suitable reactive functional groups for preparation of composites in this approach. Fu et al. [120] reported functionalization of CNTs using “grafting to” method. They refluxed CNTs containing carboxylic acid groups with thionyl chloride to convert acid groups to acylchlorides. Then, the CNTs with surface-bound acylchloride moieties were used in the esterification reactions with the hydroxyl groups of dendritic poly(polyethylene glycol) polymer. Another example of the “grafting to” approach was reported by Qin et al. [121]. They grafted SWNTs with polystyrene (PS) with functionalized end groups PS ($-\text{N}_3$), via a cycloaddition reaction. Polymer grafted CNTs were formed by covalently attaching CNTs to highly soluble linear polymers, such as poly(propionylethylenimine-co-ethylenimine) (PPEI-EI) via amide linkages or poly(vinyl acetate-co-vinyl alcohol) (PVA-VA) via ester linkages [122,123]. The resulting PVA grafted CNTs were soluble in PVA solution and PVA-CNT nanocomposites films showed very high optical quality in the “grafting from” approach. The polymer is bound to the CNTs surface by in-situ polymerization of monomers in the presence of reactive CNTs or CNTs supported initiators. The main advantage of this approach is that the polymer-CNTs composites can be prepared with high grafting density. This approach was used successfully to graft many polymers such as polyamide 6 [124,125], PMMA [126,127], PS [128,129], poly(acrylic acid) (PAA) [130], poly-(tert-butyl acrylate) [131], poly(N-isopropylacrylamide) (NIPAM) [132], poly(4-vinylpyridine) [133], and poly(N-vinylcarbazole) [134] on CNTs via radical, cationic, anionic, ring-opening, and condensation polymerizations.

CNT membranes

Types of CNT membranes

CNTs can be classified into two major categories according to the fabrication methods; (1) vertically aligned (VA) CNTs membranes, and (2) mixed matrix CNTs membranes. For VA-CNTs membranes, CNTs are arranged straight up and perpendicular to the membrane surface. In this configuration,

CNTs are bound to each other by an organic or inorganic filler material. On the other hand, mixed matrix CNTs membranes have a structure similar to that of the thin-film composite RO membranes, where the top layer is mixed with CNTs and a polymer such as polyamide (PA). Conceptual images of both CNT membranes are shown in Figure 8.3.

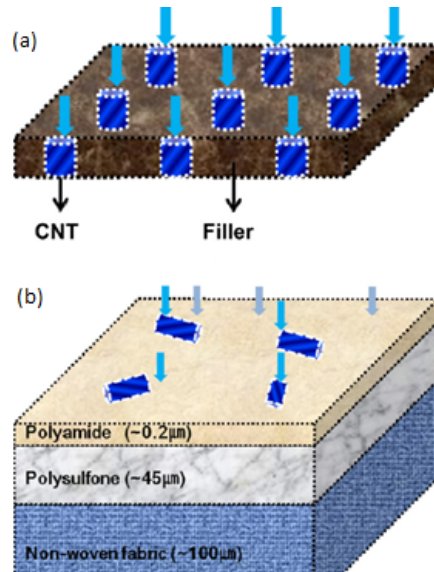


FIGURE 8.3

Conceptual structures of CNTs membranes. (a) Vertically aligned (VA) CNTs membranes, and (b) mixed matrix CNTs membranes [87]

The features of VA-CNTs membranes and mixed-CNTs membranes are summarized in Table 8.2.

TABLE 8.2

Comparison of vertically aligned (VA) CNTs membranes and mixed (composite) CNTs membranes [87]

VA CNTs membranes	Mixes CNTs membranes
<ul style="list-style-type: none"> • CNTs are aligned vertically 	<ul style="list-style-type: none"> • CNTs are mixed with polymeric materials
<ul style="list-style-type: none"> • CNTs forest is compacted densely 	<ul style="list-style-type: none"> • Composite layers with PSf membrane and non-woven support
<ul style="list-style-type: none"> • Water flux is supposed to be fast drastically 	<ul style="list-style-type: none"> • Water flux is moderately fast
<ul style="list-style-type: none"> • Functional group can be attached at the tip of CNTs or on the membrane surface conveniently 	<ul style="list-style-type: none"> • Low (or anti-) fouling membrane
<ul style="list-style-type: none"> • Fabrication procedures are complicated 	<ul style="list-style-type: none"> • Fabrication procedures are conveniently simple
<ul style="list-style-type: none"> • May need specially adjusted operating system 	<ul style="list-style-type: none"> • Operationally feasible to the conventional membrane process

One important advantage of VA-CNTs membranes is that water flux should be very rapid due to the short nano-channel length and compactness of the CNT forest. The VA-CNTs membrane was initially attempted due to the nanofluidics, but fabrication made it difficult to produce the large quantities needed for commercialization. Meanwhile, the mixed-CNTs membrane has its own merits such as relatively simple manufacturing procedure and similarity to existing membrane processes. Therefore, more attention seems to be given to mixed-CNTs membranes.

Vertically aligned CNTs membranes

The first prototype for a VA-CNTs membrane was introduced by Hinds's research group [135]. After being grown on an iron catalyst using the CVD process, MWNTs were embedded in polymeric filler composed of polystyrene (PS). Hinds and coworkers performed a series of supplementary pressure-driven flow experiments with the MWNTs/PS membrane and found that water flow rate increases 4- to 5-fold over those of conventional fluid flow, which was estimated from the Hagen–Poiseuille equation [136]. Originally, the Hinds's research group developed the CNTs membrane as a chemically selective gate keeper, which could separate different sized enzymes [137]. Thus, they did not report ion selectivity, which is strongly related to desalination potential during desalination process. Based on a moderate inner diameter (I.D. = ~ 7 nm), they conjectured that its salt rejection capability might not be very high. In addition, Holt et al. developed a micro-electro mechanical system compatible fabrication process for another type of VA-CNTs membrane [138] which employs CNTs with an inner diameter < 2 nm (average I.D. = 1.6 ± 0.4 nm) to enhance the nanofluidic effect. Inorganic filler (silicon nitride, Si_3N_4) was employed to ensure that water flows only through the nano-channels and does not permeate through the nanotube-filler matrix. Holt and his collaborators reported that water fluxes are > 3 -fold greater than those of non-slip hydrodynamic flow as calculated using the Hagen–Poiseuille equation [138]. The major features of the two representative VA-CNTs membrane studies for water treatment are compared in Table 8.3.

TABLE 8.3

Major features of vertically aligned (VA) CNT membranes [87]

Research group	Hinds group	Holt group
Pros	<ul style="list-style-type: none"> • Polymer (i.e., polystyrene) was used as a filler material • Relatively simple fabrication procedure • Good reproducibility of empirical data 	<ul style="list-style-type: none"> • CNT membrane with ultrafine pores (< 2nm) • Inorganic filler matrix (Si_3N_4) • MEMS fabrication process • Good permeability without free volume and leakage • Enhanced ion selectivity (high desalination potential)
Cons	<ul style="list-style-type: none"> • Poor ion selectivity with MWCNTs • Distribution of irregular pore sizes 	<ul style="list-style-type: none"> • Complicated fabrication process • Additional procedure needed (e.g., back etching)

Mixed (composite) CNTs membranes

An earlier model of a mixed-CNTs membrane was mainly designed to upgrade a UF membrane with nanotubes. MWNTs (up to 5% by weight) were blended with polysulfone (PSf), and water fluxes were measured under an operating pressure of 1–4 bar [139]. Intriguingly, the MWNT/PSf membrane revealed two pieces of conflicting data according to the molecular weight of solute. For an aqueous solution of poly-ethyleneoxide 100,000, the solute rejection efficiency was high (>95%) and water flux was measured at 14–17 L m⁻² h⁻¹ (LMH). In contrast, the solute rejection efficiency was reduced by 20–60% for an aqueous solution of poly-vinylpyrrolidone (PVP) 55,000, whereas water flux was >40 LMH. Choi et al. presumed that the plugging effect between both sizes of the nano-pores and the solute molecules may contribute to differences in the solute rejection efficiencies [34]. Thus, it seems to be a dilemma to accomplish higher permeability and rejection rate at the same time with the mixed-CNTs membrane. Functionalized MWNTs blended with PSf were also prepared for UF membranes [140]. MWNTs were modified by attaching isocyanate and isophthaloyl chloride functional groups, and protein adsorption on the membrane surface was suppressed. Thus, it was anticipated that a functionalized MWNT/PSf membrane would alleviate the membrane biofouling. Additionally, a mixed-CNT membrane for RO process has a water flux of 4.05 LMH/bar [141]. Compared to a commercialized brackish water (BW) RO membrane whose normalized water flux ranged from 2.5 to 3.0 LMH/bar, the mixed-CNTs membrane demonstrated ~1.5-fold higher normalized water flux. However, a number of issues should be resolved, which are addressed in the following section.

Fabrication of CNTs membranes

Since CNTs have found their potential for fluid transport, there has been continuous interest in developing methods for CNTs fillings and decorations. Although the existing simulations and experimental studies have provided substantial evidence that can be constructively used to produce membranes with high flux and high selectivity, it is difficult to synthesize CNTs with well-controlled length below 100nm [142]. It was found that, there are many different properties which can be manipulated in different ways, depending on dispersion and alignment of CNTs in polymermatrix when processing these nanocomposites. To date, the efforts made towards these challenges have been remained. It is generally acceptable that some form of post-processing of CNTs is required prior to their incorporation into polymeric composites in order to prevent aggregation and ensure the CNTs are homogeneously and individually dispersed throughout the matrixes. The tailored CNTs membranes are normally constructed of chemically opened CNTs that are arranged in close-packed structures [143].

The ideal membrane structure can be obtained by filling the spaces between the CNTs with a continuous polymeric film and etching the closed ends of the CNTs [144]. The interfacial wetting and bonding between CNTs and polymer matrix can be improved via surface functionalization of CNTs in order to create strong CNTs array–polymer interface adhesion between the surrounding polymer chains. On the other hand, funtionalization has also been shown to drastically affect flux of the transported particles through the resulting CNTs-membranes. These findings demonstrated that it is possible to control and tune the molecular transport properties of CNTs-membranes in a systematic fashion.

Alignment and filling of CNTs

Advances in nanoporous CNTs-membranes design with improved properties as composite materials such as chemical selectivity and flux can be attained via the incorporation and alignment of CNTs within a polymer film to form a well-ordered membrane structure as illustrated in Figure 8.4. Development of effective techniques to align CNTs in polymer matrixes is a crucial point to be achieved as the alignment has a direct effect on performance of CNTs-membranes in terms of physical properties such as mechanical strength and their flux and selectivity. Unfortunately, due to the extremely flexible and high aspect ratio of CNTs, it is very difficult to align the CNTs using ordinary composite fabrication methods [145]. Various approaches have been reported to prepare aligned CNTs arrays, using both physical and chemical methods [146]. It is worth mentioning that, the dimension compatibility of CNTs and the polymeric chains enable the development of simple procedures and make the experimental conditions easy to prepare CNTs membrane composites with desired properties. As demonstrated by the work carried out by Chen and Tao [147], the relaxation and alignment of polyurethane (PU) chains during the swelling and moisture curing stages give rise to the penetration of polar solvent tetrahydrofuran (THF) and are believed to serve as the driving force for the assembly of the oriented CNTs in the polymer. The alignment of SWCNTs in PU during the polar solvent casting process is illustrated in Figure 8.5.

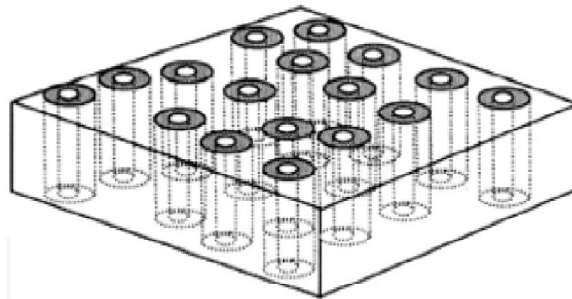


FIGURE 8.4

Schematic of the target CNTs-MMM structure in which the pores being the rigid inner-tube diameter of the CNTs

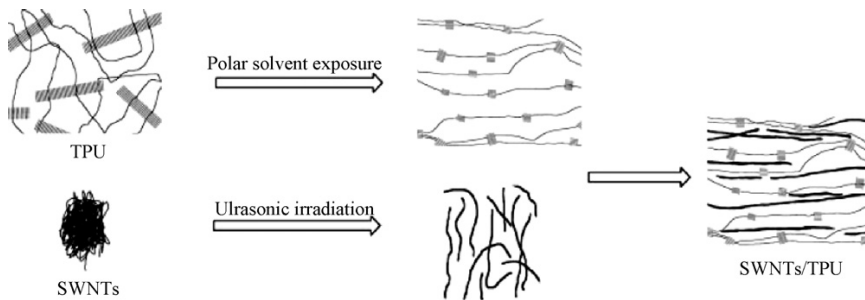


FIGURE 8.5

Schematic illustration of the alignment of SWCNTs in PU during polar solvent casting process [21]

It is impossible to synthesize CNTs based membranes with the CNTs inter-grown together without

inter-tube gaps due to the unique structures of CNTs and their growth mechanism. Therefore, filling the inter-CNTs gaps and removal of the polymer over-layer are important in the synthesis of aligned CNTs membrane. Polystyrene (PS) has been experimentally proven to have high wettability with CNTs and therefore, it is expected that the CNT arrays are readily impregnated with PS [148-151]. The pioneer successful work on filling CNTs with PS was reported by Liu et al. [151], who employed supercritical CO₂ for encapsulation of MWCNTs with outer diameter of 40–50 nm, in which the filling fraction can be controlled to some extent by changing the release time. However, the filling of PS is also strongly dependent on the structure of CNTs. For example, it has been noticed that the bamboo-like CNTs structure with closed compartment could serve as barrier that prohibits penetration of monomer molecules. The selective filling of CNTs can be carried out via controlling the size of flexible polymer molecules, wherein the low molecular weight polymers are allowed to pass through the CNT channels, while transport of the high molecular weight polymers are restricted by their size to enter the cavities of CNTs [152].

A breakthrough in the synthesis of vertically aligned MWCNTs array in fabrication of CNTs-membranes has been reported by Hinds et al. [148] via filling the inter-tube gaps with PS by spin coating method. The resulting freestanding composite films, with the CNTs alignment intact from top to bottom of the polymer films, were of 5–10 μm thickness. Due to this arrangement, the ends of the aligned CNTs were accessible to the outer molecules from both sides of the formed membranes. Therefore, it is very possible to utilize the hollow inner cavities of the CNTs for separation applications. The H₂O plasma-enhanced oxidation was performed to remove the thin layer of excess polymer from the top surface and the CNTs tips were opened to form the membrane structure. The micrograph in Figure 8.6 illustrates the cleaved edge of the CNTs-PS membrane after plasma oxidation. The CNT tips were 10-50nm above the polymer surface as the plasma oxidation could etch PS faster than CNTs.

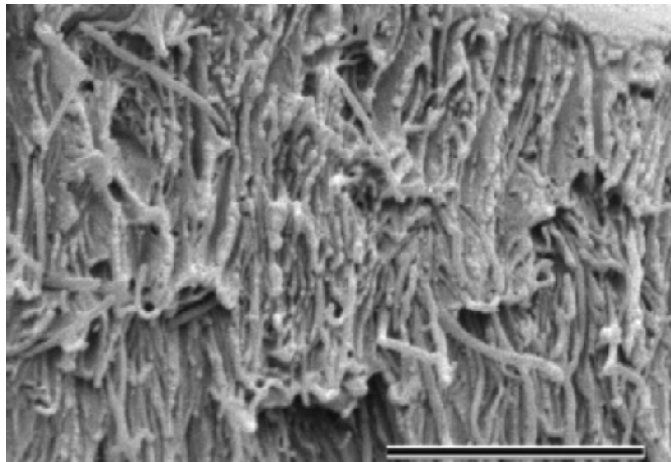


FIGURE 8.6

Micrograph of the cleaved edge of CNTs-PS membranes after exposure to plasma oxidation [21]

Similarly, Mi et al. [150] reported an alignment method using a porous alumina support. The vertically aligned MWCNTs were grown supported via a multi-step method, i.e. growth of vertical CNTs by chemical vapor deposition (CVD) followed by filling the inter-CNTs gaps with PS by spin coating to form PS-filled CNTs with thickness of about 20 μm. PS completely covered the surface

and did not penetrate deeply into the alumina support pores due to the hydrophobic affinity demonstrated by CNTs which allowed PS to stay mainly within the CNTs layer. Similarly, Tofighy et al. [50] used chemical vapor deposition (CVD) method for synthesis of vertically aligned MWCNTs films with thickness of about 10-15 μm on macroporous surface of α -alumina support using cyclohexanol and ferrocene as carbon source and catalyst, respectively. Then as-grown vertically aligned MWCNTs were oxidized using HNO_3 and H_2SO_4 and then employed as membrane in desalination process (sodium chloride removal from water). Cross sectional SEM image of the vertically aligned MWCNTs film on macroporous surface of α -alumina support prepared by Tofighy et al. is shown in Figure 8.7.

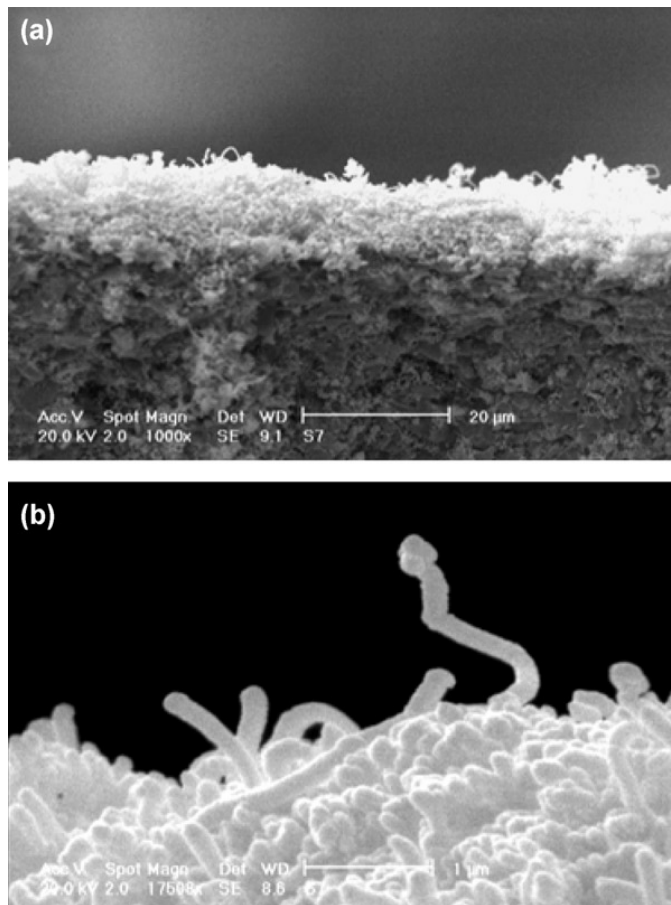


FIGURE 8.7

(a) Cross sectional SEM image of vertically aligned MWCNTs film on macroporous surface of α -alumina support, (b) high magnification SEM image of the vertically aligned MWCNTs film [50]

FTIR spectrum of the oxidized CNTs membrane prepared by Tofighy et. al. is shown in Figure 8.8. As can be observed, acid treatment process introduces many functional groups onto the surface of oxidized CNTs membrane: hydroxyl groups (3500cm^{-1}), carboxyl groups (1650cm^{-1}), and carbonyl groups (1400cm^{-1}), which can provide a large number of chemical adsorption sites onto the surface of the oxidized CNTs membrane.

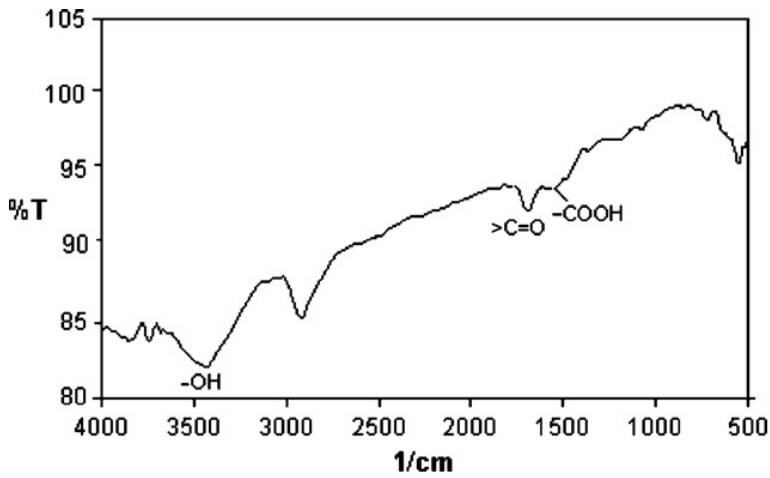


FIGURE 8.8
FTIR spectrum of the oxidized CNTs membrane [50]

Nanostructure of a CNT from the CNTs film before and after acid treatment is shown in Figure 8.9a and b, respectively (TEM images). As can be observed, acid treatment can remove metallic particles trapped in the CNTs.

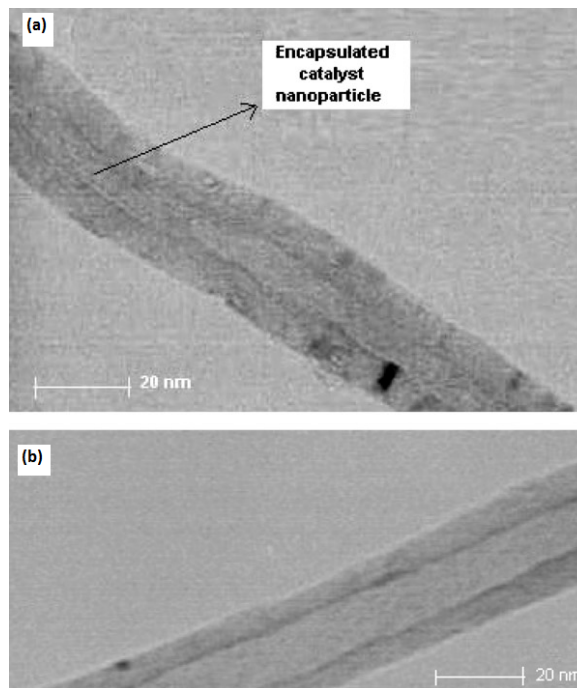


FIGURE 8.9
TEM image of a typical CNT (a) before acid treatment and (b) after acid treatment [50]

Oxidation etching was commonly utilized to purify and create open end termini in the structure to

produce shorter, and more distinct and one-end uncapped CNTs, which were required to form a regular array of CNTs [153]. Because of the presence of impurities in the as-grown CNTs, purification was required during the process. Plasma etching is the method of choice for purification as it does not damage the highly desirable vertical aligned CNTs in membranes. The unique layered structure of impurities such as dense packed amorphous carbon films that are formed on the top of aligned CNTs can be selectively removed as this amorphous carbon layer is more susceptible to the plasma etching than the CNTs. Micrographs in Figure 8.10 show that the CNTs tips which are more reactive than tube walls are found to be opened after plasma etching of the perpendicularly aligned CNTs. As an alternative to avoid the expensive equipment required for plasma etching, mechanical polishing and acid treatment were applied to remove PS over the layer and to open the closed tips of CNTs [150].

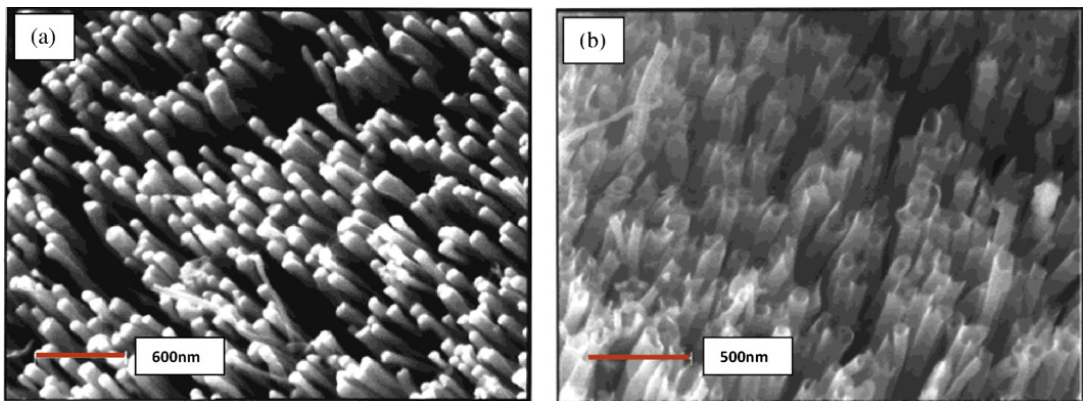


FIGURE 8.10

SEM images of the aligned CNTs (a) before and (b) after the plasma-treatment followed by gently washing with HCl (37%) to remove the Fe catalyst residues [153]

Functionalization and grafting of CNTs

Due to the presence of van der Waals force, CNTs tend to form stabilized bundles which in turn results in the formation of tight bundles [154]. Furthermore, the relatively smooth CNTs surfaces which lack interfacial bonding have limited the load transferring from the matrix to the CNTs [155]. By introducing some functional groups to the CNTs, it is possible to obtain homogeneous and fine dispersion of CNTs in the polymer matrix and simultaneously activate the CNTs surfaces by creating active functional groups such as carboxyl or hydroxyl groups [156,157]. Generally, CNTs-MMMs possess large areal density of graphitic cores having entrances that can be functionalized by molecules of desired length, hydrophobicity or chemical functionality. The most conventionally and commonly used functionalization method is via surface treatment with strong acids [158]. The acid modified CNTs have hydroxyl and carboxyl groups at their open ends and defect sites, enabling them to make good dispersion in various polar organic solvents. Furthermore, presence of these functional groups developed at the open ends and the defect sites of the CNTs may induce some form of interaction with the polymer. However, the harsh reaction condition may also result in significant damages and defects to the structure of CNTs, which in turn leads to adverse impacts on physical properties such as mechanical strength and thermal resistance. Therefore, chemical modification should be carried out in properly controlled manner in order to preserve the CNT

structure and generate sufficient functional groups onto the CNTs. On the other hand, noncovalent functionalization by functional polymers and large organic molecules has shown to be a promising technique to improve solubility and compatibility of CNTs in organic solvents. Advantage of this method is that structure and original properties of the CNTs remain unchanged after modification. CNTs can be easily functionalized using cyclodextrin (CD) treatment. The CD modification of CNTs is both simple and effective. It requires no prolonged heating, filtration and washing which can severely damage the small diameter CNTs. Chen et al. showed that CD has superior CNT-dispersing capability and provides an excellent pathway to dispersion of CNTs in organic matrix through disentanglement of the CNTs' bundles.

Deng et al. [159] performed a three-step surface treatment of MWCNTs to enhance dispersion of the CNTs in poly(ether urethane) (PEU). Carboxylation and hydroxylation of the MWCNTs were carried out via chemical treatment using mixed strong acids and thionyl chloride/1,6-hexanediol respectively. The functionalized MWCNTs were then treated via isophorone diisocyanate (IPDI) to obtain MWCNTs grafted IPDI (Figure 8.11). Well dispersed MWCNTs in PEU matrix just by simple solution blending were demonstrated. In addition, functional groups such as phenylamine [160], chlorobenzoic acid [161] and acyl chloride [162] were also found to be readily reacted with CNTs. The functionalization is likely to occur along the length and at the tips of CNTs in which higher degree of functionalization is expected to take place at the tips where reactivity is much higher. The presence of these functional groups significantly enhances surface area and interfacial adhesion between the polymer matrix and CNTs. Nevertheless, introduction of mutually interactive functional groups on the polymer and CNTs may lead to pore channel partial blockage, thus hindering separation performance. Therefore, it is desired to modify the CNTs surface to increase the polymer compatibility without affecting the pore structure [163].

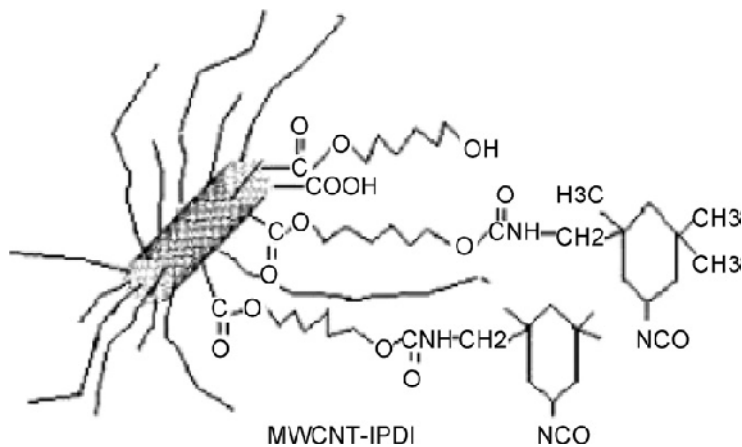


FIGURE 8.11

MWCNTs IPDI grafted via a multi-steps modification [159]

Besides enhancing the compatibility between the CNTs and polymer, functional groups attached to the pore surfaces can also lead to highly selective separations by forcing a chemical interaction between permeating molecules and the functional molecules. The opened CNTs tips in the membranes are terminated with functional groups that can be easily derivatized with molecules that bind to bulky receptors, modifying the entrance of the CNTs pores, and this hence can be used to control the pores entrance of the CNTs-embedded membranes [164]. It is an important

consideration that the molecules bound to the CNTs pores should be small enough to avoid self-blockage at the core of the pores. The plasma oxidation during the membrane fabrication process introduced carboxylic acid groups on the CNTs tips that could be readily reacted with other biomolecules or functionalizing molecules and thus offered a unique nanoscale system allowing gatekeeper chemical interactions [148]. With proper functionality, transport through hydrophobic CNTs cores would be similar to biological membrane channels. Majumder et al. [165] reported an experimental procedure for chemical functionalization of CNTs membranes. Simple carbodiimide chemistry was performed on the plasma edged CNTs with desired functional molecules containing accessible amine. The configuration of functional molecules is important for controlling flow and selectivity of chemical transport which occur near the CNTs tip entrances and not along the entire length of the CNTs, consistent with gatekeeper geometry.

The similar gatekeeper mechanism was applied by drawing tethered molecules that are charged to the entrances of the CNTs cores to produce voltage gated channels [166]. The functional density on the CNTs was increased via electrochemical grafting of the diazonium compounds in order to provide a measurable response of voltage gated transport through CNTs-MMMs. During the grafting process, not only the tips, but also the interior cores of the CNTs were functionalized. On the other hand, the interior cores were masked from the reaction by having a fast velocity core flow of inert solution. Since the grafted molecules at the entrances of CNTs can sterically hinder larger molecules and the charged ligands are found to enhance diffusivity of the oppositely charged permeates, this principle can be applied to mimic the mechanism of ion channels to the selective transport of permeating molecules across the membrane.

CNTs for separation

The application of CNTs as membrane filler in fabrication of MMMs has been recognized for some time. As discussed in the earlier section, the examinations on the transport properties through CNT pores or channels have shown that CNTs-MMMs are predicted to have spectacularly high flux using MD computational simulations, hence illustrating the potential of this class of membranes to be used in separation applications. Through the proper fabrication controls such as alignment, filling and functionalization of CNTs to provide good interface interaction during the formation of CNTs-MMMs, it is possible for CNTs to demonstrate enhanced and promising results in their transport properties. Since the experimental realization of MMMs made up of CNTs performed by Hind et al. [148], a number of related works have been reported. MMMs based on CNTs dispersed inside polymeric matrixes have been well developed and characterized for separation applications.

Gas separation by CNTs membranes

It was proposed that adding inorganic fillers can affect gas separation in two ways. Firstly, the strong interaction between polymer chains and nanofillers may disrupt the polymer chain packing and increase the voids and thus significantly enhance the gas diffusion; secondly, the functional groups on the surface of inorganic filler phase may interact with some gases to improve their solubility in the MMMs. Separation of the fillers out of the membrane matrix or formation of the separated filler phases due to gravity or incompatibility during fabrication of MMMs may also deteriorate their gas separation performance. However, in a recent study [167], it was been reported based on gas transport mechanism that the increased gas diffusivity and permeability is not only due to the gas transportation inside the channels of inorganic fillers, but also due to the

presence of narrow gaps or voids which create shorter alternative routes that enable the gas molecules to pass through easily. In fact, the gas transport of MMMs that occurs through non-selective voids between the matrix walls and the sieve particles has also been proposed by other researchers [168,169]. Therefore, depending on the features of the resulting MMMs, such as compatibility of the polymer and the inorganic filler, transport properties of the MMMs can be varied.

In order to apply CNTs-MMM practically in a wide range of gas separation, a better understanding of gas diffusion on the pore surface and through the pores channel of CNTs-MMMs could be achieved by conducting a well-controlled investigation of gas interactions with the membranes [170]. It is an interesting subject to study, as the CNT surface is suggested to be responsible and plays a very influential role in the molecular transport mechanism, which determines the potential of these CNTs-MMMs for use in gas separation applications. Surface physisorption type of interaction in CNTs in composite structures is very important, particularly for the larger tubes where size exclusion does not occur, and it can be advantageous for high selectivity and flux in membranes. Vibrational spectroscopy such as Raman spectroscopy [170] is very useful for the in situ membrane characterization as the molecular vibrations are sensitive to their local environment. Moreover, the adsorption geometry and interaction between the gases and the CNTs-MMMs are capable of perturbing molecular vibrations and shows some shifting features with different degrees, depending on the type of molecules. However, the failure in observing shiftings for physisorbed molecules results from small Raman cross section or low coverage. Therefore, computational modelings of diffusion in these composite membranes are required to capture and provide accurate simulation findings.

Skoulidas et al. [171] applied atomistic simulations to study CO₂ adsorption in SWCNTs at room temperature as a function of their diameters. Linear and spherical models of CO₂ were compared; however, the adsorption isotherms were qualitatively very similar. On the other hand, diffusivities increased with decreasing nanotube diameter due to the increased smoothness of the solid–fluid potential energy surface. Diffusion of N₂ was also studied through a model of SWCNTs membranes with thickness of 5 μm and surface area of $3.1 \times 10^{-4} \text{ m}^2$. The molecular diffusivities in CNTs are orders of magnitude larger than those in zeolites, and also considerably larger than that predicted based on Knudsen diffusion. However, when a real CNT membrane is applied experimentally, presence of defects, blockage of CNTs at some interstitial and exterior sites by impurities or residual functional groups and transport resistance resulted by pores entrance and exit effects have to be taken into account as these factors may contribute to remarkable decrease in diffusivities and permeability of gas molecules [172]. The differences are especially obvious when ultra-thin membranes are considered.

Similarly, the atomically detailed simulation was also used to examine performance and effectiveness of CNTs-MMMs in separating gas mixtures. Sholl et al. [173] performed a computational calculation for permeation of CH₄/H₂ mixture through a detailed model of CNTs membrane constructed from close packed bundles of SWCNTs that were observed experimentally. The adsorption selectivity of molecules inside the CNTs is greatly driven by the different interaction potentials of the molecules with the graphitic carbon. At pressure relevant to practical applications, the CNTs showed the stronger adsorption selectivity for CH₄ over H₂ due to the stronger interaction of CH₄ with the pores wall, which also suggested that H₂ has larger saturation capacity than CH₄. It is in general consent that the transport resistances associated with molecular entering and exiting the CNTs COULD be neglected if the membranes used were sufficiently thick when compared to other thin nanoporous membranes, therefore, in the conducted experiments, the adsorbate concentrations at the boundaries of the membranes were defined from the binary adsorption

isotherm. Another important observation of extremely rapid diffusion rate of molecules inside CNTs, arising from the extraordinary smoothness of the potential-energy surface, can be contributed to the predicted flux that is orders of magnitude larger for individual pores, differentiating them in important ways from polymeric and zeolitic membranes.

Theoretical performance of CNTs-MMMs based on diffusivities and fluxes in SWCNTs predicted by Sholl et al. was further verified by Kim and his co-workers [174]. High diffusion coefficients of gases such as O₂, N₂ and CH₄ in CNTs-MMMs based on open-ended CNTs indicated the presence of high diffusivity of CNT tunnel within poly(imide siloxane) matrix. They reported that permeability values for O₂, N₂ and CH₄ increase in proportion to the amount of CNTs added to the polymer matrix.

Addition of 10 wt% CNTs resulted in an increase from 11.99 to 17.83 Barrers, 28.19 to 36.7 Barrers and 32.24 to 39.81 Barrers for permeability of N₂, CH₄ and O₂, respectively. The nearly endless and highly entangled carbon ropes were cut into shorter length and the tube ends were opened via acid treatment as the addition of closed end CNTs would act as impermeable filler and lower down permeability of gases through the channel. It was identified that impenetrable volumes and rigidifying elements within polymer matrixes reduce diffusivity of gas molecules to different extents, depending on the size of molecules [175]. It is generally known that the presence of unselective voids at the interface between polymer and CNTs offers sites of high permeability for He. Therefore, the significant reduction in permeability of He observed confirms that the polymer adheres well to the CNTs due to the presence of siloxane component that has good wetting properties on the graphite surface. In another similar study [172], where SWCNTs were incorporated within PSF matrix to enhance its gas transport performance, increasing both permeability and diffusivity for H₂, O₂, CH₄ and CO₂ was reported. For all the gases, the separation factors were found to be mainly dependant on the CNTs content rather than the effect of interfacial zone which consists of constrained polymer segments. Adsorption isotherms for CH₄ shown in Figure 8.12 imply that the amount of gas adsorbed in the CNT-MMMs system is significantly influenced by the CNTs content. On the other hand, influences of both the CNTs content and the presence of voids surrounding CNTs on gas permeability were also observed. Cong et al. [167] reported that when the functionalized MWCNTs are orientated vertically to the membrane surface, they act as pinholes that allow CO₂ and N₂ molecules to pass through rapidly and higher gas permeability is achieved by increasing the CNTs content and through formation of the nanogaps surrounding CNTs.

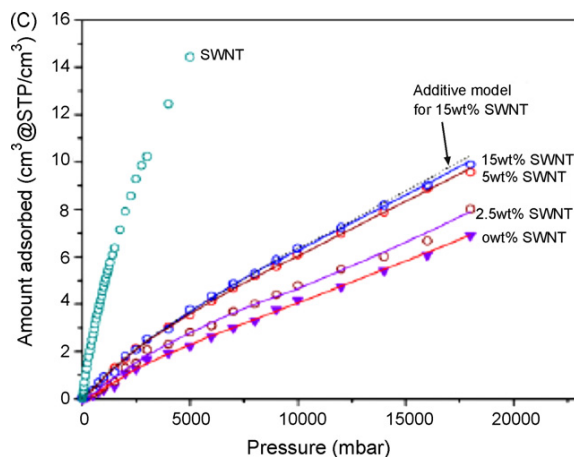


FIGURE 8.12

Adsorption isotherms of functionalized SWCNT/PSF MMMs for CH₄ with different CNTs loadings [172]

Gilani et. al. [176] reported separation of methane-nitrogen mixtures using synthesized vertically aligned CNTs membranes. In this work, capabilities of CNTs membranes fabricated in cylindrical pores of anodic aluminum oxide (AAO) substrate to separate the binary mixtures of CH_4/N_2 were studied experimentally. For this purpose, the permeability and selectivity of three CNT/AAO membranes with different growth time as 6, 12 and 18 h were investigated. CNTs were grown vertically through holes of AAO by CVD of acetylene gas. Study on permeability and selectivity of membranes for three binary mixtures of CH_4/N_2 showed that when the CNT inner diameters are 34 and 24 nm, viscous flow is the governing mechanism and insignificant selectivities of 1.2–1.24 are achieved. However, the membrane with CNT inner diameter and wall thickness of 8 and 16 nm respectively is considerably selective for CH_4 over N_2 . It was also found that CH_4 mole fraction in feed and upstream feed pressure has major effects on permeability and selectivity. The membrane with 18 h synthesis time exhibited the selectivity in the range of 1.8–3.85. The enhancement factor for N_2 single gas diffusivity was also found to be about three times larger than that predicted by Knudsen diffusion model (Figures 8.13-8.15).

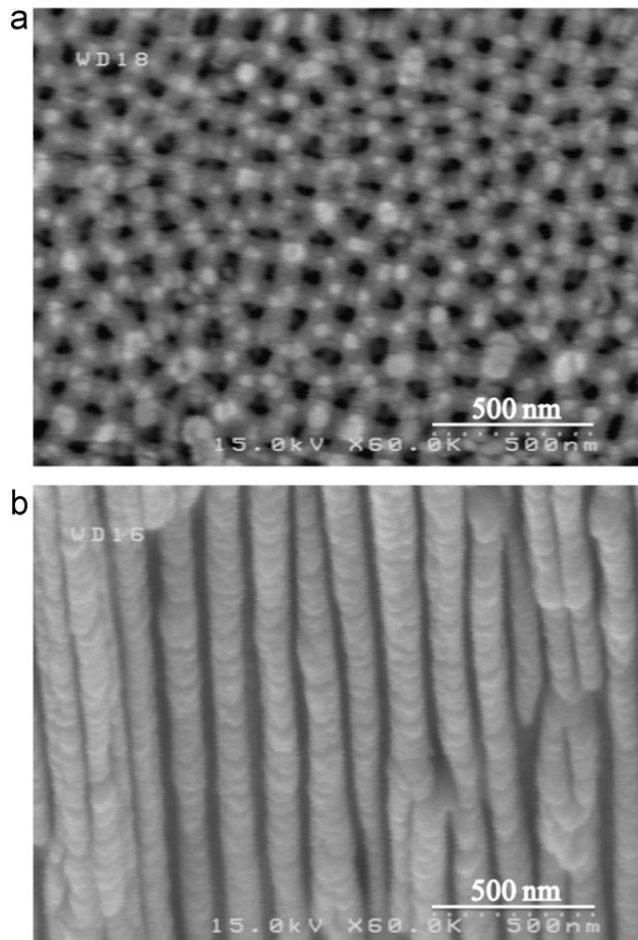
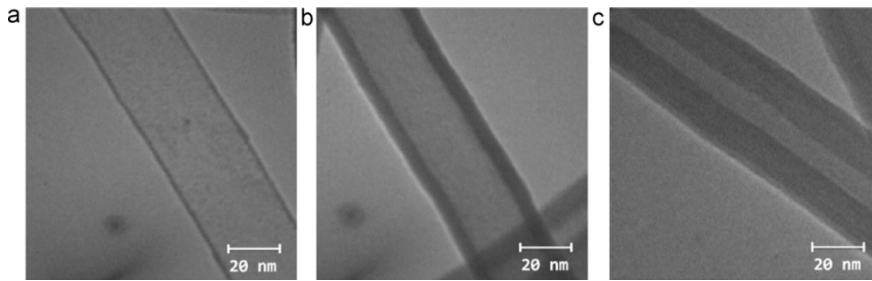
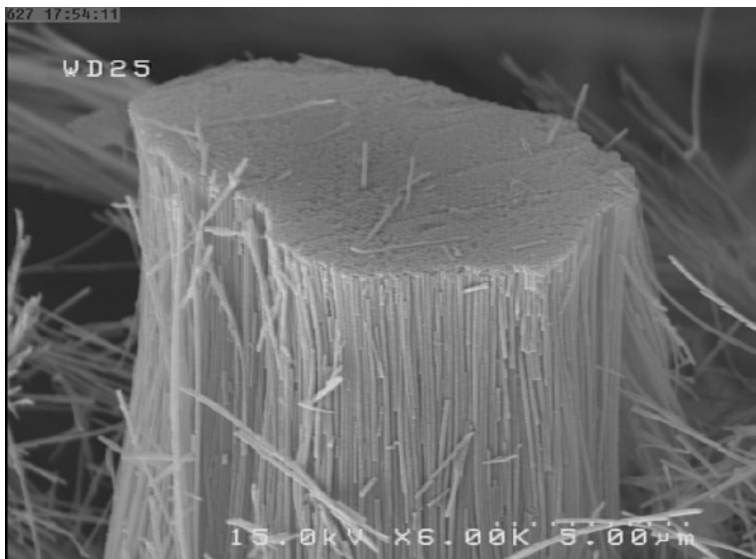


FIGURE 8.13

(a) FESEM image of AAO substrate prepared by anodization process. (b) Cross section FESEM image of AAO [176]

**FIGURE 8.14**

TEM images of MWCNTs in different CVD synthesis times: (a) M1, (b) M2, and (c) M3 [176]

**FIGURE 8.15**

FESEM image of VA-CNTs after removing AAO from M3 membrane [176]

Liquid separation and pervaporation (PV) by CNTs membranes

A vast number of publications have been reported on separation of liquids using CNTs, however, most of the findings reported based on theoretical calculations obtained from using simulation models.

CNTs membranes were simulated to compare their efficiency with existing semi permeable membranes used for water desalination via reverse osmosis [177]. By tuning size and uniformity of the CNTs, desired salt rejection without having trade-off against permeation flux could be obtained. When non polar CNTs with narrow pore diameter are used, it is possible to allow permeation of water molecules through the pores but not ions. The ions face a large energy barrier hindering their entrance to the narrow pores while water requires little or no energy for the entry due to the formation of stable hydrogen bonds. However, in order to realize the application of CNTs-membranes for water desalination, the CNTs are required to be packed within a solid nonporous

material to prevent them from separating apart so that a CNTs-membrane that is stable under large hydrostatic pressure can be obtained.

Despite those simulation studies, the practical application of CNTs-membranes in liquid separation and pervaporation has been scarcely reported. To date, only a few studies have been conducted to examine the potential of the CNTs-membranes for this purpose.

Pervaporation performance of the resulting MWCNT incorporated polyvinyl alcohol (PVA) membranes was carried out, by Choi et al. [158]. As those general trends observed in other membrane performance studies, increasing total flux of MWCNT-PVA membranes and decreasing selectivity of a water/ethanol (10/90 wt%) mixture with increasing MWCNTs content were reported. These phenomena can be attributed to the effects of two key factors: crystallinity of the membrane and molecular transport through the CNTs. Higher the MWCNTs contents creates strong interaction with PVA and therefore prevents packing of the molecules to form crystals, resulting in a reduced crystallinity of the PVA matrix. As a result, the polymer matrix is more accessible to the penetrates and hence their permeabilities increase. In addition, due to the smaller molecular size, ethanol and water molecules can transport across the inner cores of the CNTs. With increasing the MWCNTs content, more diffusion of penetrates takes place and this hence contributes to higher permeation flux as observed from the trend depicted in Figure 8.16.

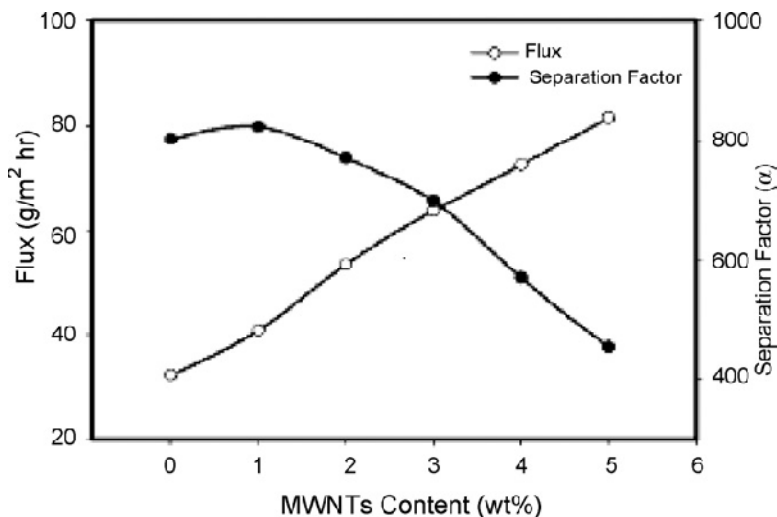


FIGURE 8.16

Total permeation flux and separation factor of the MWCNTs/PVA membrane in separation of water/ethanol (10/90 wt%) as a function of MWCNTs contents [158]

In a similar research, Peng et al. [178] studied pervaporation properties of CNTs-PVA membranes for separation of benzene/cyclohexane mixtures. The CNTs were dispersed in cyclodextrin by grinding during formation of the membranes in order to reduce aggregation and improve compatibility of CNTs in the polymer matrix. The resulting membranes exhibited the highest benzene permeation flux of $61.0 \text{ gm}^{-2} \cdot \text{h}^{-2}$ with separation factor of 41.2 for a mixture with weight percent of 1:1. Upon comparison of pervaporation properties with the PVA and cyclodextrin dispersed PVA membranes [179], the membranes prepared through incorporation of CNTs demonstrated much better mechanical strength properties and pervaporation properties that were above the upper bound trade-off curve.

Molecules of another mixture, triisopropyl orthoformate (TIPO) and n-hexane, which are smaller than the membrane pore size, were also successfully separated by a dense CNTs membrane via pervaporation [180]. Due to the higher molecular weight of TIPO, the molecules were preferentially adsorbed and then resulting in permeability differences that enabled separation of TIPO from n-hexane. Generally, presence of higher content of CNTs in the membranes enhances permeability of the penetrates as discussed earlier.

Shirazi et. al. [181] reported synthesis and characterization of CNTs/PVA nanocomposite membranes for dehydration of isopropanol. The membrane preparation procedure is shown in Figure 8.17. In this work, CNTs were synthesized via CVD method using cyclohexanol and ferrocene as carbon precursor and catalyst, respectively (Figure 8.18). Nitric acid was used for purification and functionalization of CNTs. TEM image of CNTs before and after purification revealed that acid treatment could remove encapsulated catalyst particles as shown in Figure 8.19. Afterward, highly pure and functionalized CNTs were incorporated in PVA to synthesize PVA–CNTs nanocomposite membranes. FESEM characterization was carried out to investigate dispersion of different CNTs loading in PVA matrix. The results showed that 2 wt.% CNTs loading is better dispersed in the polymer and increasing CNTs loading more than 2 wt.% agglomerates CNTs (Figure 8.20). Degree of swelling results for the nanocomposite membranes showed that the present of CNTs in the PVA membranes reduces the degree of swelling. Furthermore, pervaporation (PV) results revealed that incorporating the CNTs in the PVA matrix increases significantly water selectivity due to rigidification of the polymer chains. The water selectivities for the neat PVA and 2 wt.% CNTs loading nanocomposite membranes were evaluated as 119 and 1794, respectively.

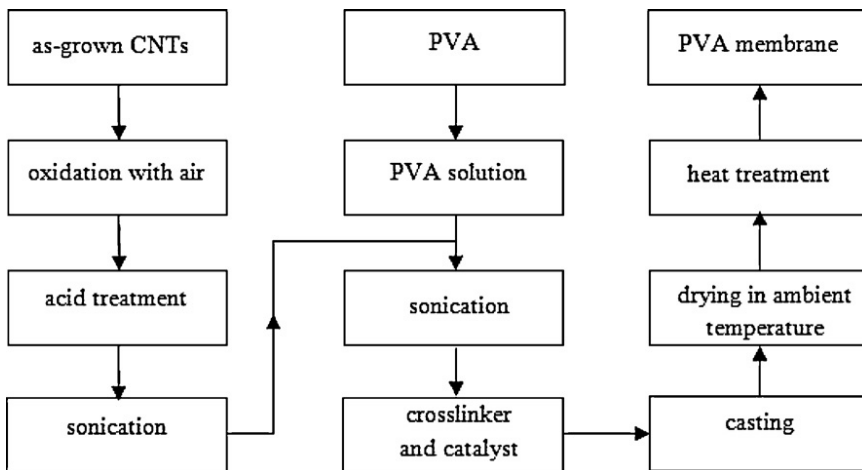


FIGURE 8.17

Membrane preparation procedure reported by Shirazi et. al. [181]

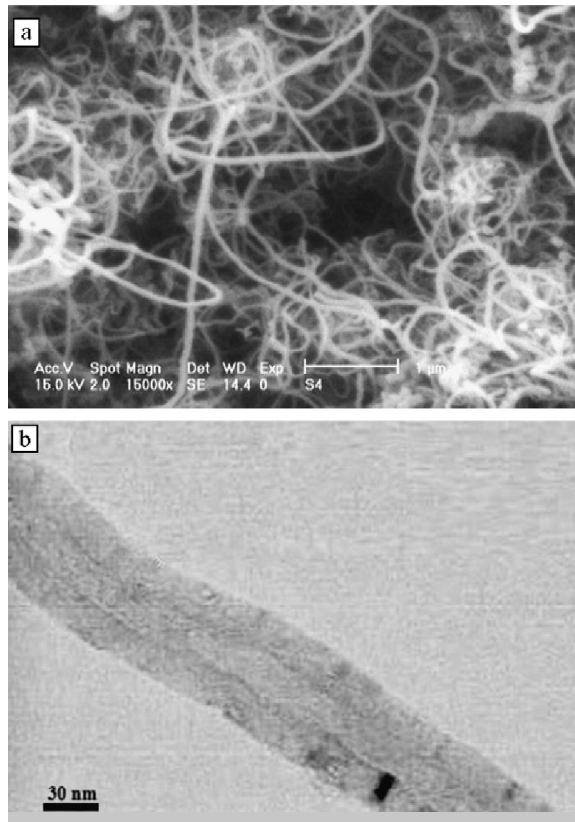


FIGURE 8.18
(a) FESEM and (b) TEM images of as-grown CNTs [181]

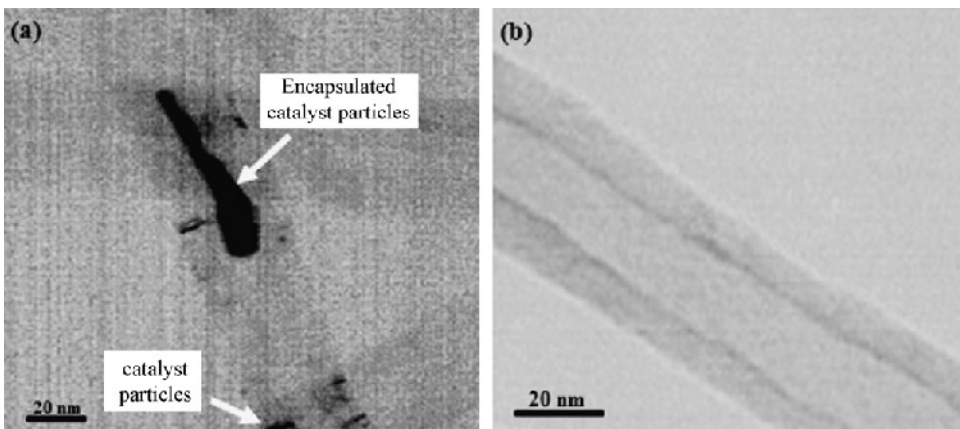
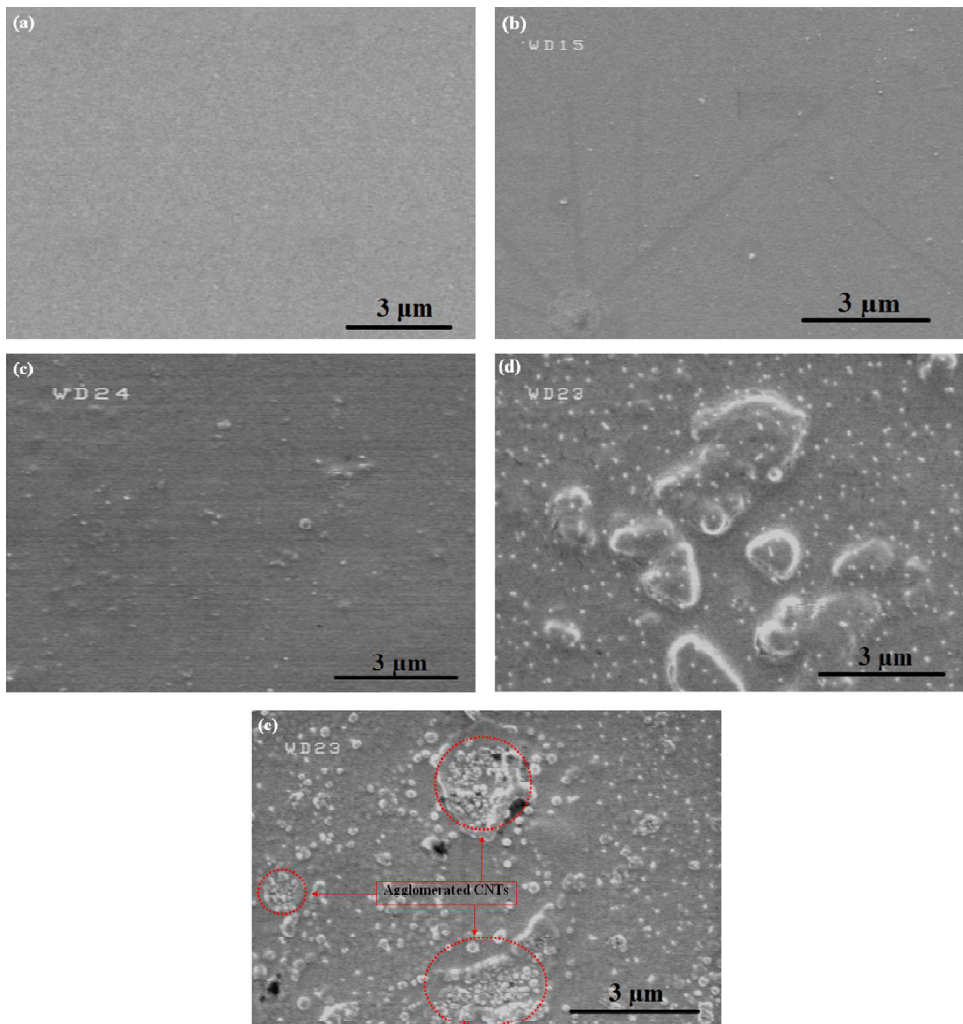


FIGURE 8.19
TEM images of (a) as-grown CNTs (b) CNTs treated by 8 M HNO₃ [181]

**FIGURE 8.20**

FESEM surface images of (a) PVA-0 (b) PVA-0.5 (c) PVA-1 (d) PVA-2 and (e) PVA-4 [181]

Amirilargani et. al. reported the effects of poly (allylamine hydrochloride) as a new functionalization agent on preparation of PVA/MWNTs membranes [182]. Using a solution technique, poly (allylamine hydrochloride)-wrapped multiwalled carbon nanotubes (MWNT-PAH) incorporated Poly (vinyl alcohol) (PVA) membranes were prepared. The prepared membranes were subjected to PV dehydration of isopropanol (IPA). Their results demonstrated that MWNTs wrapped with PAH were well dispersed in the polymer matrix in comparison with prepared MWNTs. Degree of swelling (DS) of the prepared membranes decreased by addition of MWNT-PAH into the PVA matrix. Incorporation of modified CNTs into the PVA matrix increases water selectivity significantly due to the rigidification of the polymer chains. The nanocomposite membrane containing 1 wt.% of MWNTPAH exhibited excellent PV properties. Permeation flux and separation factor were $0.229 \text{ Kg/m}^2\text{h}$ and 141.2 for the raw PVA and $0.207 \text{ Kg/m}^2\text{h}$ and 948.4 for the

membrane prepared with 1 wt.% of MWNT-PAH. Separation factor decreased significantly by further addition of MWNT-PAH due to its agglomeration in the PVA matrix (Figures 8.21-8.24).

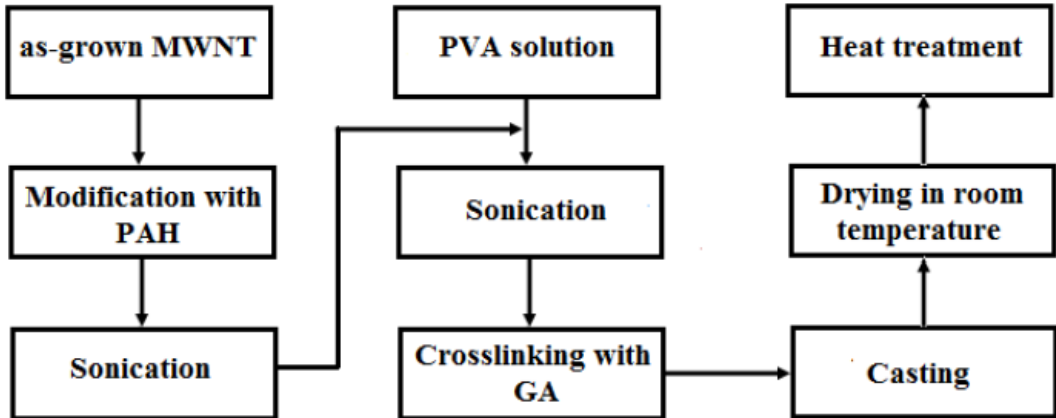


FIGURE 8.21

Preparation procedure of the PVA/MWNT-PAH nanocomposite membranes [182]

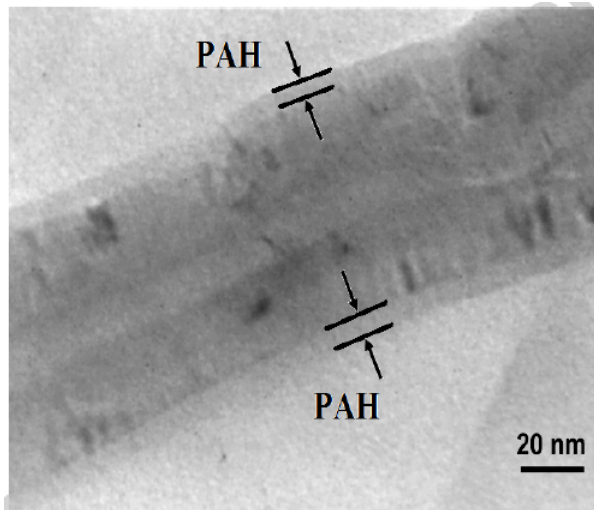


FIGURE 8.22

HR-TEM image of the PAH-wrapped MWNTs [182]

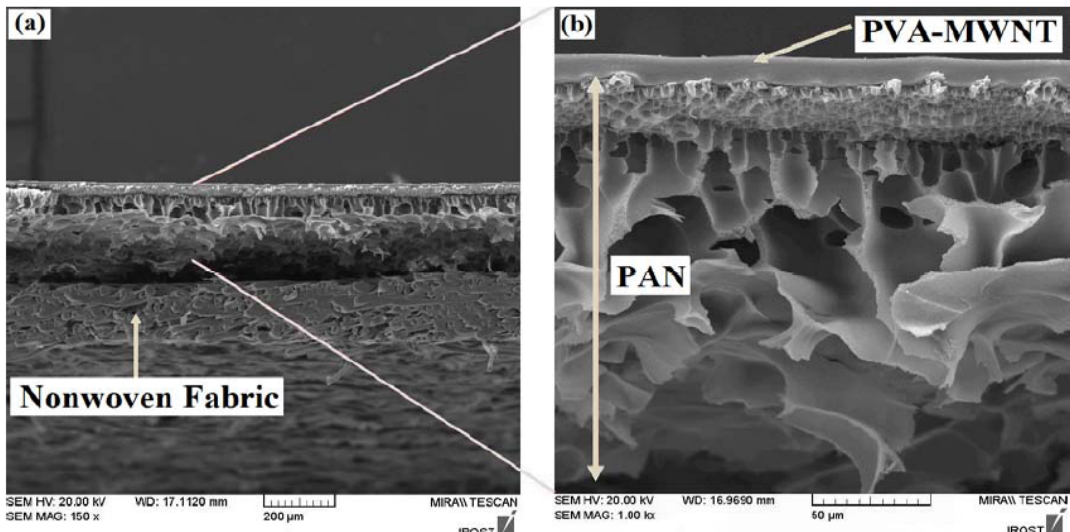


FIGURE 8.23

PVA/MWNT-PAH nanocomposite membrane on the PAN support layer [182]

However, this is not always true for all processes. Mondal and Hu [183] reported the adverse effects observed with the presence of high MWCNTs content. Functionalized MWCNTs were incorporated into segmented polyurethane (SPU) to study water vapor transport properties. In such MMM system, MWCNTs were found to influence both crystalline and amorphous regions of SPU matrix by imparting stiffness to the polymer matrix, particularly when added in excess. The increased stiffness of the polymer chains prevents the passage of water molecules through the polymer matrix. Furthermore, the permeating molecules have to experience longer tortuous path when passing through the impermeable nanoparticles. As a result, the decreasing in permeability due to increasing MWCNTs content was observed in the study.

It is in agreement that using composite CNTs in water treatment possess several potential advantages [180,184]. Previous toxicological evaluations showed that some fullerenes and CNTs might exhibit possible toxicity towards bacteria when dispersed in membranes. In a waste water treatment process, the presence of microorganism may act as foulant material that induces biofouling and eventually results in high maintenance costs. Therefore, the membranes based on CNTs might serve as a basis for mitigation of membrane fouling through inhibition of bacterial growth in the membrane water processes.

One of the considerations to be taken into account is alignment of CNTs and adhesion between CNTs and substrate, in which CNTs with uniform lengths and diameters must be firmly anchored to surface. Narayan et al. [185] successfully fabricated CNTs composite films with unusual antimicrobial properties against *S. aureus* and *S. warneri* bacteria through pulsed laser ablation of carbon. Nonetheless, immobilization of CNTs in membranes may not be able to display antibacterial activity under the unfavorable fabrication condition. The study of Brunet et al. [140] on antibacterial properties of ultrafiltration membranes made from MWCNTs-polysulfone composites showed negative results most probably due to the concentration of CNTs in the membrane skin layer and the alteration of the bioavailability resulted by the polymer wrapping phenomenon. In order to get rid of these concerns, dispersion of CNTs must be enhanced with longer mixing and compatibility of polymers can be improved through wrapping or

throughput membranes. Therefore, it is expected that CNTs-membranes may act as an additional and valuable tool for upgrading the quality of separation processes available in current market. Several experimental works have recently confirmed the theoretically predicted outstanding transport properties of CNTs in CNTs-membranes. In most of the separation studies, CNTs-Membranes have demonstrated improved separation performance and displayed attractive selectivity versus permeability characteristics. The overall enhancement in both permeability and flux for gas and liquid permeates suggests that CNTs can provide high diffusivity tunnels within the polymer matrix. Also, it is interesting to reveal that the transport properties can be further optimized through controlling of some influential key parameters such as size and loading amount of CNTs.

Since its existence, the membrane technology based on CNTs-membranes has expanded and become one of the most popular research topics due to its spectacular separation performance, particularly through the results obtained from molecular simulations. However, realization of these simulation results into practical laboratory processes still requires more activities regarding some remained technological difficulties.

References

1. S. Iijima, *Nature* 354 (1991) 56–8.
2. G. Van Lier, C. Van Alsenoy, V. Van Doren, P. Geerlings, *Chem Phys Lett* 326 (2000) 181–5.
3. M.M.J. Treacy, T.W. Ebbesen, J.M. Gibson, *Nature* 381 (1996) 678–80.
4. M.F. Yu, O. Lourie, M.J. Dyer, K. Moloni, T.F. Kelly, R.S. Ruoff, *Science* 287 (2000) 637–40.
5. A. Thess, R. Lee, P. Nikolaev, H. Dai, P. Petit, J. Robert et al., *Science* 273 (1996) 483–7.
6. Y. Ando, X. Zhao, H. Shimoyama, G. Sakai, K. Kaneto, *Int J Inorg Mater* 1 (1999) 77–82.
7. R.H. Baughman, A.A. Zakhidov, W.A. de Heer, *Carbon nanotube-the route toward applications. Science* 297 (2000) 787–92.
8. M.J. Biercuk, M.C. Llaguno, M. Radosavljevic, J.K. Hyun, A.T. Johnson, *Appl Phys Lett* 80 (2002) 2767–9
9. R.Z. Ma, J. Wu, B.Q. Wei, J. Liang, D.H. Wu, *J Mater Sci* 33 (1998) 5243–6.
10. H.L. Zhang, J.F. Lia, K.F. Yao, L.D. Chen, *J Appl Phys* 97 (2005) 114310.
11. L.M. Peng, Z.L. Zhang, Z.Q. Xue, Q.D. Wu, Z.N. Gu, D.G. Pettifor, *Phys Rev Lett* 85 (2000) 3249–52.
12. Z. Gu, Y. Yang, K. Li, X. Tao, G. Eres, J.Y. Howe et al., *Carbon* 49 (2011) 2475–82.
13. T.W. Ebbesen, P.M. Ajayan, *Nature* 358 (1992) 220–222.
14. T. Guo, P. Nikolaev, A.G. Rinzler, D. Tomanek, D.T. Colbert, R.E. Smalley, *Journal of Physical Chemistry* 99 (1995) 10694–10697.
15. J. Kong, A.M. Cassell, H.J. Dai, *Chemical Physics Letters* 292 (1998) 567–574.
16. B. Chen, P. Wu, *Carbon* 43 (2005) 3172–3177.
17. W.S. Winston Ho, K.K. Sirkar, Chapter 1: Overview, in: W.S. Winston Ho, K.K. Sirkar (Eds.), *Membrane Handbook*, Chapman & Hall, New York, London, 1992, pp. 3–15.
18. M. Mulder, Chapter 1: Introduction, in: M. Mulder (Ed.), *Basic Principle of Membrane Technology*, Kluwer Academic Publisher, Dordrecht/Boston/ London, 1991, pp. 1–15.
19. W. Eykamp, Chapter 1: Microfiltration and ultrafiltration, in: R.D. Noble, S.A. Stern (Eds.), *Membrane Science and Technology Series, 1, Membrane Separations Technology: Principles and Applications*, Elsevier Science, B.V., 1995, pp. 1–40.

20. R.W. Baker, Chapter 1: Overview of membrane science and technology, in: R.W. Baker (Ed.), *Membrane Technology and Applications*, 2nd Edition, John Wiley & Sons Ltd, 2004, pp. 1–14.
21. A.F. Ismail, P.S. Goh, S.M. Sanip, M. Aziz, *Separation and Purification Technology* 70 (2009) 12–26.
22. C.J. Vrolijk, P. Green, J. Salisbury, R.B. Lammers, *Science* 289 (2000) 284.
23. M.A. Shannon, P.W. Bohn, M. Elimelech, J.G. Georgiadis, B.J. Marinas, A.M. Mayes, *Nature* 452 (2008) 301.
24. J. Glater, *Desalination* 117 (1998) 297.
25. M. Elimelech, W.A. Phillip, *Science* 333 (2011) 712.
26. H. Ludwig, *Desalination and Water Treatment* 13 (2010) 13.
27. GWI, *Desalination Markets 2005–2015*, GWI, Oxford, 2004.
28. C. Fritzmann, J. Löwenberg, T. Wintgens, T. Melin, *Desalination* 216 (2007) 1.
29. R. Semiat, *Environmental Science & Technology* 42 (2008) 8193.
30. O.M. Al-Hawaj, *Desalination and Water Treatment* 8 (2009) 131.
31. B.J. Hinds, N. Chopra, T. Rantell, R. Andrews, V. Gavalas, L.G. Bachas, *Science* 303 (2004) 62.
32. M. Majumder, N. Chopra, R. Andrews, B.J. Hinds, *Nature* 438 (2005) 44.
33. M. Majumder, P. Ajayan, *Comprehensive Membrane Science and Engineering* 1 (2010) 291.
34. G. Hummer, J.C. Rasaiah, J.P. Noworyta, *Water conduction through the hydrophobic channel of a carbon nanotube*, *Nature* 414 (2001) 188.
35. A.I. Kolesnikov, J.-M. Zanotti, C.-K. Loong, P. Thiyagarajan, A.P. Moravsky, R.O. Loutfy, C.J. Burnham, *Phys. Rev. Lett.* 93 (2004) 35503.
36. N. Naguib, H. Ye, Y. Gogotsi, A.G. Yazicioglu, C.M. Megaridis, M. Yoshimura, *Nano Lett.* 4 (2004) 2237.
37. Y. Maniwa, Y. Maniwa, K. Matsuda, H. Kyakuno, S. Ogasawara, T. Hibi, H. Kadowaki, S. Suzuki, Y. Achiba, H. Kataura, *Nat. Mater.* 6 (2007) 135.
38. E. Mamontov, C.J. Burnham, S.H. Chen, A.P. Moravsky, C.K. Loong, N.R. de Souza, A.I. Kolesnikov, *J. Chem. Phys.* 124 (2006) 194703.
39. A. Waghe, J.C. Rasaiah, G. Hummer, *J. Chem. Phys.* 117 (2002) 10789.
40. A. Kalra, S. Garde, G. Hummer, *Proc. Natl. Acad. Sci. U.S.A.* 100 (2003) 10175–10180.
41. E.M. Kotsalis, J.H. Walther, P. Koumoutsakos, *Int. J. Multiphase Flow* 39 (2004) 995.
42. I. Hanasaki, A. Nakatani, *J. Chem. Phys.* 124 (2006) 144708.
43. A. Striolo, *Nano Lett.* 6 (2006) 633.
44. A.I. Skoulidas, D.M. Ackerman, J.K. Johnson, D.S. Sholl, *Phys. Rev. Lett.* 89 (2002) 185901.
45. B.J. Hinds, N. Chopra, R. Rantell, R. Andrew, V. Gavalas, L.G. Bachas, *Science* 303 (2004) 62.
46. J.K. Halt, H.G. Park, Y.M. Wang, M. Stadermann, A.B. Artyukhin, C.P. Grigoropoulos, A. Noy, Q. Bakajin, *Science* 312 (2006) 1034.
47. W. Mi, J.Y.S. Lin, Y. Li, B. Zhang, *Synthesis of vertically aligned carbon nanotube films on macroporous alumina substrates*, *Mesopor. Micropor. Mater.* 81 (2005) 185–189.
48. W. Mi, Y.S. Lin, Y. Li, *J. Membr. Sci.* 304 (2007) 1–7.
49. F. Fornasiero, H.G. Park, J.K. Holt, M. Stadermann, C.P. Grigoropoulos, A. Noy, O. Bakajin, *PNAS* 105 (2008) 17250–17255.
50. M. Ahmadzadeh Tofighy, Y. Shirazi, T. Mohammadi*, Afshin Pak, *Chemical Engineering Journal* 168 (2011) 1064–1072.

51. A. Bachtold, P. Hadley, T. Nakanishi, C. Dekker, *Science* 294 (2001) 1317–20.
52. H. Ago, K. Petritsch, M.S.P. Shaffer, A.H. Windle, R.H. Friend, *Adv Mater* 11 (1999) 1281–5.
53. A.Y. Kasumov, R. Deblock, M. Kociak, B. Reulet, H. Bouchiat, I. Khodos et al., *Science* 284 (1999) 1508–11.
54. R.H. Baughman, C. Cui, A.A. Zakhidov, Z. Iqbal, J.N. Barisci, G.M. Spinks et al., *Science* 284 (1999) 1340–4.
55. C. Niu, E.K. Sichel, R. Hoch, D. Moy, H. Tennet, *Appl Phys Lett* 70 (1997) 1480–2.
56. P.M. Ajayan, S. Iijima, *Nature* 361 (1993) 333–4.
57. X.L. Xie, Y.W. Mai, X. Ping, *Mater Sci Eng Rep* 49 (2005) 89–112.
58. R. Andrews, M.C. Weisenberger, *Solid State Mater Sci* 8 (2004) 31–7.
59. S. Iijima, T. Ichihashi, *Nature* 363 (1993) 603–5.
60. D.S. Bethune, C.H. Kiang, M.S. Devries, G. Gorman, R. Savoy, J. Vazquez et al., *Nature* 363 (1993) 605–7.
61. T. Sugai, H. Yoshida, T. Shimada, T. Okazaki, H. Shinohara, *Nano Lett* 3 (2003) 769–73.
62. S. Bandow, M. Takizawa, K. Hirahara, M. Yudasaka, S. Iijima, *Chem Phys Lett* 337 (2001) 48–54.
63. T. Guo, P. Nikolaev, A. Thess, D.T. Colbert, R.E. Smalley, *Chem Phys Lett* 243 (1995) 49–54.
64. P. Nikolaev, M.J. Bronikowski, R.K. Bradley, F. Rohmund, D.T. Colbert, K.A. Smith et al., *Chem Phys Lett* 313 (1999) 91–7.
65. M. Joseyacaman, M. Mikiyoshida, L. Rendon, J.G. Santiesteban, *Appl Phys Lett* 62 (1993) 657–9.
66. S.M. Huang, M. Woodson, R.E. Smalley, J. Liu, *Nano Lett* 4 (2004) 1025–8.
67. M.M. Treacy, T.W. Ebbesen, J.M. Gibson, *Nature* 381 (1996) 678–80.
68. R. Saito, G. Dresselhaus, M.S. Dresselhaus, *Physical properties of carbon nanotubes*. London: Imperial College Press; 1998.
69. H.G. Chae, J. Liu, S. Kumar, *Carbon nanotubes properties and applications*. In: O'Connell MJ, editor. *Carbon nanotube-enabled materials*. Boca Raton: Taylor & Francis Group, LLC; 2006.
70. C. Ma, W. Zhang, Y. Zhu, L. Ji, R. Zhang, N. Koratkar et al., *Carbon* 46 (2008) 706–10.
71. P.M. Ajayan, L.S. Schadler, P.V. Braun, *Nanocomposite science and technology*. Weinheim, Germany: Wiley-VCH, GmbH & Co. KGaA; 2003.
72. J.P. Lu, *Phys Rev Lett* 79 (1997) 1297–300.
73. Y. Li, K. Wang, J. Wei, Z. Gu, Z. Wang, J. Luo et al., *Carbon* 43 (2005) 31–5.
74. M.F. Yu, O. Lourie, M.J. Dyer, K. Moloni, T.F. Kelly, R.S. Ruoff, *Science* 287 (2000) 637–40.
75. X.L. Xie, Y.W. Mai, X.P. Zhou, *Materials Science and Engineering R* 49 (2005) 89–112.
76. A. Thess, R. Lee, P. Nikolaev, H. Dai, P. Petit, J. Robert, C. Xu, Y.H. Lee, S.G. Kim, A.G. Rinzler, *Science* 273 (1996) 483.
77. B. Corry, *The Journal of Physical Chemistry B* 112 (2008) 1427.
78. G. Hummer, J.C. Rasaiah, J.P. Noworyta, *Nature* 414 (2001).
79. J. Köfinger, G. Hummer, C. Dellago, *Proceedings of the National Academy of Sciences* 105 (2008) 13218.
80. T.A. Hilder, D. Gordon, S.H. Chung, *Small* 5 (2009) 2183.
81. J.A. Thomas, A.J.H. McGaughey, *Nano Letters* 8 (2008) 2788.
82. J.K. Holt, *Advanced Materials* 21 (2009) 3542.
83. A. Striolo, *Nano Letters* 6 (2006) 633.

84. A. Ismail, P.S. Goh, S. Sanip, M. Aziz, *Separation and Purification Technology* 70 (2009) 12.
85. C. Lee, S. Baik, *Carbon* 48 (2010) 2192.
86. K. Sears, L. Dume´ e, J. Schu¨ tz, M. She, C. Huynh, S. Hawkins, M. Duke, S. Gray, *Materials* 3 (2010) 127.
87. C.H. Ahn, Y. Baek, C. Lee, S.O. Kim, S. Kim, S. Lee, S.H. Kim, S.S. Bae, J. Park, J. Yoon, *Journal of Industrial and Engineering Chemistry* 18 (2012) 1551–1559.
88. A. Hirsch, *Angew Chem Int Ed* 41 (2002) 1853–9.
89. H.S. Nalwa, editor. *Handbook of nanostructured materials and nanotechnology*, vol. 5. New York: Academic Press; 2000.
90. T.W. Ebbesen, P.M. Ajayan, H. Hiura, K. Tanigaki, *Nature* 367 (1994) 519–1519.
91. H. Hiura, T.W. Ebbesen, K. Tanigaki, *Adv Mater* 7 (1995) 275–6.
92. A. Kuznetsova, D.B. Mawhinney, V. Naumenko, J.T. Yates, J. Liu, R.E. Smalley, *Chem Phys Lett* 321 (2000) 292–6.
93. J. Liu, A.G. Rinzler, H. Dai, J.H. Hafner, R.K. Bradley, P.J. Boul et al., *Science* 280 (1998) 1253–6.
94. S. Niyogi, M.A. Hamon, H. Hu, B. Zhao, P. Bhowmik, R. Sen et al., *Acc Chem Res* 35 (2002) 1105–13.
95. H. Park, J. Zhao, J.P. Lu, *Nano Lett* 6 (2006) 916–9.
96. X. Zhang, T.V. Sreekumar, T. Liu, S. Kumar, *J Phys Chem B* 108 (2004) 16435–40.
97. J.W. Cho, J.W. Kim, Y.C. Jung, N.S. Goo, *Macromol Rapid Commun* 26 (2005) 412–6.
98. V. Georgakilas, K. Kordatos, M. Prato, D.M. Guldi, M. Holzinger, A. Hirsch, *J Am Chem Soc* 124 (2002) 760–1.
99. Y. Zhang, Z. Shi, Z. Gu, S. Iijima, *Carbon* 38 (2000) 2055–9.
100. V. Datsyuk, M. Kalyva, K. Papagelis, J. Parthenios, D. Tasis, A. Siokou et al., *Carbon* 46 (2008) 833–40.
101. Bandow S, Rao AM, Williams KA, Thess A, Smalley RE, Eklund PC., *J Phys Chem B* 101 (1997) 8839–42.
102. G.S. Duesberg, M. Burghard, J. Muster, G. Philipp, *Chem Commun* (1998) 435–6.
103. J.I. Paredes, M. Burghard, *Langmuir* 20 (2004) 5149–52.
104. G.S. Duesberg, J. Muster, V. Krstic, M. Burghard, S. Roth, *Appl Phys A* 67 (1998) 117–9.
105. V.C. Moore, M.S. Strano, E.H. Haroz, R.H. Hauge, R.E. Smalley, J. Schmidt et al., *Nano Lett* 3 (2003) 1379–82.
106. M.F. Islam, E. Rojas, D.M. Bergey, A.T. Johnson, A.G. Yodh, *Nano Lett* 3 (2003) 269–73.
107. J. Chen, A.M. Rao, S. Lyuksyutov, M.E. Itkis, M.A. Hamon, H. Hu et al., *J Phys Chem B* 105 (2001) 2525–8.
108. I. Vasiliev, S.A. Curran, *J Appl Phys* 102 (2007) 1–5.
109. O. Zhou, R.M. Fleming, D.W. Murphy, C.H. Chen, R.C. Haddon, A.P. Ramirez et al., *Science* 263 (1994) 1744–7.
110. E.T. Mickelson, C.B. Huffman, A.G. Rinzler, R.E. Smalley, R.H. Hauge, J.L. Margrave, *Chem Phys Lett* 296 (1998) 188–94.
111. E.T. Mickelson, I.W. Chiang, J.L. Zimmerman, P.J. Boul, J. Lozano, J. Liu et al., *J Phys Chem B* 103 (1999) 4318–22.
112. K.F. Kelly, I.W. Chiang, E.T. Mickelson, R.H. Hauge, J.L. Margrave, X. Wang et al., *Chem Phys Lett* 313 (1999) 445–50.
113. P.J. Boul, J. Liu, E.T. Mickelson, C.B. Huffman, L.M. Ericson, I.W. Chiang et al., *Chem Phys Lett* 310 (1999) 367–72.

114. J.L. Bahr, E.T. Mickelson, M.J. Bronikowski, R.E. Smalley, J.M. Tour, *Chem Commun* (2001) 193–4.
115. M Holzinger, O. Vostrowsky, A. Hirsch, F. Hennrich, M. Kappes, R. Weiss et al. *Angew Chem Int Ed* 40 (2001) 4002–5.
116. J.L. Bahr, J. Yang, D.V. Kosynkin, M.J. Bronikowski, R.E. Smalley, J.M. Tour, *J Am Chem Soc* 123 (2001) 6536–42.
117. J.L Bahr, J.M. Tour, *Chem Mater* 13 (2001) 3823–4.
118. J.B. Baek, C.B. Lyons, L.S. Tan, *Macromolecules* 37 (2004) 8278–85.
119. Z. Jin, X. Sun, G. Xu, S.H. Goh, W. Ji, *Chem Phys Lett.* 318 (2000) 505–10.
120. K. Fu, W. Huang, Y. Lin, L.A. Riddle, D.L. Carroll, Y.P. Sun, *Nano Lett.* 1 (2001) 439–41.
121. S. Qin, D. Qin, W.T. Ford, D.E. Resasco, J.E. Herrera, *Macromolecules* 37 (2004) 752–7.
122. J.E. Riggs, Z. Guo, D.L. Carroll, Y.P. Sun, *J Am Chem Soc* 2000 122 (2000) 5879–80.
123. Y. Lin, B. Zhou, K.A.S. Fernando, P. Liu, L.F. Allard, Y.P. Sun, *Macromolecules* 36 (2003) 7199–204.
124. L. Qu, L.M. Veca, Y. Lin, A. Kitaygorodskiy, B. Chen, A.M McCall et al., *Macromolecules* 38 (2005) 10328–31.
125. M. Yang, Y. Gao, H. Li, A. Adronov, *Carbon* 45 (2007) 2327–33.
126. S.J. Park, M.S. Cho, S.T. Lim, H.J. Cho, M.S. Jhon, *Macromol Rapid Commun* 24 (2003) 1070–3.
127. Z. Yao, N. Braidy, G.A. Botton, A. Adronov, *J. Am. Chem. Soc.*125 (2003) 16015–24.
128. D. Baskaran, J.W. Mays, M.S. Bratcher, *Angew Chem Int Ed* 43 (2004) 2138–42.
129. H. Kong, C. Gao, D. Yan, *Macromolecules* 37 (2004) 4022–30.
130. H. Kong, P. Luo, C. Gao, D. Yan, *Polymer* 46 (2005) 2472–85.
131. H. Kong, C. Gao, D. Yan, *J Mater Chem*14 (2004) 1401–5.
132. H. Kong, W. Li, C Gao, D. Yan, Y. Jin, D.R.M. Walton et al. , *Macromolecules* 37 (2004) 6683–6.
133. S. Qin, D. Qin, W.T. Ford, J.E. Herrera, D.E. Resasco, *Macromolecules* 37 (2004) 9963–7.
134. W. Wu, S. Zhang, Y. Li, J. Li, L. Liu, Y. Qin et al. , *Macromolecules* 36 (2003) 6286–8.
135. B.J. Hinds, N. Chopra, T. Rantell, R. Andrews, V. Gavalas, L.G. Bachas, *Science* 303 (2004) 62.
136. M. Majumder, N. Chopra, R. Andrews, B.J. Hinds, *Nature* 438 (2005) 44.
137. M. Majumder, N. Chopra, B.J. Hinds, *ACS Nano* 5 (2011) 3867.
138. J.K. Holt, H.G. Park, Y. Wang, M. Stadermann, A.B. Artyukhin, C.P. Grigoropoulos, A. Noy, O. Bakajin, *Science* 312 (2006) 1034.
139. J.H. Choi, J. Jegal, W.N. Kim, *Journal of Membrane Science* 284 (2006) 406.
140. S. Qiu, L. Wu, X. Pan, L. Zhang, H. Chen, C. Gao, *Journal of Membrane Science* 342 (2009) 165.
141. T.V. Ratto, J.K. Holt, A.W. Szmodis, *Membranes with embedded nanotubes for selective permeability*, Google Patents, 2011.
142. C. Klinke, J.M. Bonard, K. Kern, *Phys. Rev. B* 71 (3) (2005) 1–7.
143. D.S. Sholl, *Chem. Phys. Lett.* 305 (3–4) (1999) 269–275.
144. R.W. Baker, K. Lokhandwala, *Ind. Eng. Chem. Res.* 47 (2008) 2109–2121.
145. J.H. Sung, H.S. Kim, H.-J. Jin, H.-J. Choi, I.-J. Chin, *Macromolecules* 37 (26) (2004) 9899–9902.
146. R. Cervini, G.P. Simon, M. Ginic-Markovic, J.G. Matisons, C. Huynh, S. Hawkins, *Nanotechnology* 19 (17) (2008) 175602.

147. W. Chen, X. Tao, *Macromol. Rapid Commun.* 26 (2005) 1763–1767.
148. B.J. Hinds, N. Chopra, T. Rantell, R. Andrews, V. Gavalas, L.G. Bachas, *Science* 303 (2004) 62–65.
149. C. Matranga, B. Bockrath, N. Chopra, B.J. Hinds, R. Andrews, *Langmuir* 22 (2006) 1235–1240.
150. W. Mi, Y.S. Lin, Y. Li, *J. Membr. Sci.* 304 (1–2) (2007) 1–7.
151. Z. Liu, X. Dai, J.X.B. Han, J. Zhang, Y. Wang, Y. Huang, G. Yang, *Carbon* 42 (2) (2004) 458–460.
152. A.V. Bazilevsky, K. Sun, A.L. Yarin, C.M. Megaridis, *Langmuir* 23 (2007) 7451–7455.
153. S. Huang, L. Dai, *J. Phys. Chem. B* 106 (2002) 3542–3545.
154. V. Georgakilas, A. Bourlino, D. Gournis, T. Tsoufis, C. Trapalis, A. Mateo-Alonso, M. Prato, *J. Am. Chem. Soc.* 130 (27) (2008) 8733–8740.
155. M. Abdalla, D. Dean, D. Adibempe, E. Nyairo, P. Robinson, G. Thompson, *Polymer* 48 (2007) 5662–5670.
156. K.-S. Moon, W. Lin, H. Jiang, H. Ko, L. Zhu, C.P. Wong, *Proceedings-Electronic Components and Technology Conference*, (2008) 234–237.
157. A. Curullil, F. Valentini, S. Orlanducci, E. Tamburri, M.L. Terranova, S.N. Cesarol, G. Palleschi, *4th IEEE Conference on Nanotechnology*, (2004) 524–526.
158. J.-H. Choi, J. Jegal, W.N. Kim, *Macromol. Symp.* (2007) 610–617.
159. J. Deng, X. Zhang, K. Wang, H. Zou, Q. Zhang, Q. Fu, *J. Membr. Sci.* 288 (1–2) (2007) 261–267.
160. P. Kalappa, J.-H. Lee, J. Rashmi, T.V. Venkatesha, K.V. Pai, W. Xing, *IEEE Trans. Nanotechnol.* 7 (2) (2008) 223–228.
161. I.-Y. Jeon, H.-J. Lee, Y.-S. Choi, L.-S. Tan, J.-B. Baek, *Macromolecules* 41 (2008) 7423–7432.
162. W. Zhou, Z.-J. Du, Y.-X. Liu, X. Yang, H.-Q. Li, C. Zhang, *Compos. Sci. Technol.* 68 (15–16) (2008) 3259–3264.
163. T.W. Pechar, S. Kim, B. Vaughan, E. Marand, V. Baranauskas, J. Riffle, H.K. Leong, M. Tsapatsis, *J. Membr. Sci.* 277 (1–2) (2006) 210–218.
164. P. Nednoor, N. Chopra, V. Gavalas, L.G. Bachas, B.J. Hinds, *Chem. Mater.* 17 (14) (2005) 3595–3599.
165. M. Majumder, N. Chopra, B.J. Hinds, *J. Am. Chem. Soc.* 127 (25) (2005) 9062–9070.
166. M. Majumder, X. Zhan, R. Andrews, B.J. Hinds, *Langmuir* 23 (16) (2007) 8624–8631.
167. H. Cong, J. Zhang, M. Radosx, Y. Shen, *J. Membr. Sci.* 294 (1–2) (2007) 178–185.
168. M. Anson, J. Marchese, E. Garis, N. Ochoa, C. Pagliero, *J. Membr. Sci.* 243 (2004) 19–28.
169. W.A.W. Rafizah, A.F. Ismail, *J. Membr. Sci.* 307 (2008) 53–61.
170. C. Matranga, B. Bockrath, N. Chopra, B.J. Hinds, R. Andrews, *Langmuir* 22 (2006) 1235–1240.
171. A.I. Skoulidas, D.S. Sholl, J.K. Johnson, *J. Chem. Phys.* 124 (5) (2004) 1–7, 054708.
172. S. Kim, L. Chen, J.K. Johnson, E. Marand, *J. Membr. Sci.* 294 (1–2) (2007) 147–158.
173. H. Chen, D.S. Sholl, *J. Membr. Sci.* 269 (2006) 152–160.
174. S. Kim, T.W. Pechar, E. Marand, *Desalination* 192 (1–3) (2006) 330–339.
175. T.-S. Chung, S.S. Chan, R. Wang, Z. Lu, C. He, *Journal of Membrane Science* 211 (2003) 91–99.
176. N. Gilani, J. Towfighi Daryan, A. Morad Rashidi, M. Omidkhah, *Applied Surface Science* 258 (2012) 4819–4825.

177. J. Caro, M. Noack, *Microporous Mesoporous Mater.* 115 (2008) 215–233.
178. B. Corry, *J. Phys. Chem. B* 112 (5) (2008) 1427–1434.
179. F. Peng, C. Hu, Z. Jiang, *J. Membr. Sci.* 297 (2007) 236–242.
180. S.J. Lue, S.H. Peng, *Journal of Membrane Science* 222 (2003) 203–217.
181. M. Yu, H.H. Funke, J.L. Falconer, R.D. Noble, *Nano Lett.* 9 (1) (2009) 225–229.
182. Y. Shirazi, M. Ahmadzadeh Tofighy, T. Mohammadi, *Journal of Membrane Science* 378 (2011) 551–561.
183. M. Amirilargani, A. Ghadimi, M. Ahmadzadeh Tofighy, T. Mohammadi, *J. Membr. Sci.* 447 (2013) 315–324.
184. S. Mondal, J.L. Hu, *Polym. Eng. Sci.* 48 (9) (2008) 1718–1724.
185. M.J. O’Connell, P. Boul, L.M. Ericson, C. Huffman, Y. Wang, E. Haroz, C. Kuper, J. Tour, K.D. Ausman, R.E. Smalley, *Chem. Phys. Lett.* 342 (2001) 265–271.
186. R.J. Narayan, C.J. Berry, R.L. Brigmon, *Mater. Sci. Eng. B* 123 (2005) 123–129.